NATIONAL ADVISORY COMMITTEE
FOR AERONAUTICS

TECHNICAL NOTE 2901

AN ANALYSIS OF THE FACTORS AFFECTING THE LOSS IN LIFT AND

SHIFT IN AERODYNAMIC CENTER PRODUCED BY THE DISTORTION

OF A SWEPT WING UNDER AERODYNAMIC LOAD

By Charles W. Mathews and Max C. Kurbjun

Langley Aeronautical Laboratory
Langley Field, Va.

NACA

R

NATIONAL ADVISORY COMMITTEE FOR AERONAUTICS

TECHNICAL NOTE 2901

AN ANALYSIS OF THE FACTORS AFFECTING THE LOSS IN LIFT AND

SHIFT IN AERODYNAMIC CENTER PRODUCED BY THE DISTORTION

OF A SWEPT WING UNDER AERODYNAMIC LOAD

By Charles W. Mathews and Max C. Kurbjun

SUMMARY

A simplified analysis has been made of the factors affecting the loss in lift and the shift in aerodynamic center of a swept wing due to its distortion under aerodynamic load. The manner in which these particular aeroelastic effects influence the longitudinal stability of an airplane has been considered.

The results show that large variations in the aeroelastic effects associated with wing bending are produced by changes in aspect ratio, sweep angle, and thickness ratio. These variations are, in general, larger than those produced in wing-bending stress and with the thickness ratios being contemplated today restrict the aspect ratio to low values for large angles of sweep and, conversely, restrict the sweep angles to low values for large aspect ratios. Expressions obtained for the ratio of angle-of-attack change due to wing torsion to angle-of-attack change due to wing bending show that torsion effects tend to alleviate the effects of bending, but the angle-of-attack changes due to torsion are much smaller than those due to bending except for wings with low values of sweep, aspect ratio, or, in particular, a combination of the two. Decreasing the plan-form taper ratio is another means for extending the combinations of sweep and aspect ratio without an increase in wing structural weight. When aeroelastic considerations are important, a more rapid increase in the structural weight of wings with increase in airplane size appears to occur than for designs based on stress alone. The choice of steel or duralumin as a structural material is not significant insofar as aeroelastic considerations are concerned.

Some alleviation of aeroelastic effects occurs in maneuvers because of the inertia of the wing. In addition, the effect of the wing-aerodynamic-center shift on the longitudinal stability of an airplane with a horizontal tail may be alleviated to some extent by the compensating effect of the wing loss in lift provided the percentage reduction in wing-lift-curve slope is greater than that of the tail-lift-curve slope.
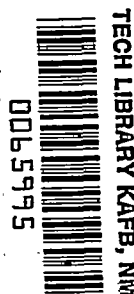
INTRODUCTION

One of the primary objectives in airplane design is the attainment of efficient high-speed performance. This objective, however, must be compromised in order to meet other requirements such as satisfactory stability and control characteristics and structural integrity. In recent years the trend has been toward the use of swept wings as a means for obtaining efficient performance at transonic speeds, but the use of swept wings has introduced a structural design problem not inherent in unswept wings. This structural design problem is a consequence of the necessity for restricting the changes in longitudinal stability of a swept-wing airplane caused by the wing bending under load.

The importance of this aeroelastic phenomenon has been recognized for some time, and several investigators have developed more or less refined methods for analysis of wing elastic distortions and their effects. (For examples, see refs. 1 to 4.) More specific evidence as to the influence of wing external geometry (in conjunction with flight condition) on this flexibility—longitudinal-stability problem would appear to be of interest to the aerodynamicist, however, so that he can obtain rough indications as to which wing plan forms would be practical from aeroelastic considerations. Accordingly, a simplified analysis has been made of the factors affecting the loss in lift and the shift in aerodynamic center of a swept wing caused by its distortion under load. A shell type of wing structure is assumed and the method of analysis obtains direct algebraic solutions for the extreme-fiber stress and the aeroelastic effects in terms of the wing structural weight and material, its external geometry, and the flight condition under which it operates. Initially, the effects of wing bending alone are considered and the effects of torsion are included subsequently through determination of the ratio of angle-of-attack changes resulting from wing torsion to those resulting from wing bending. The solutions are presented in the form of parametric charts which, in turn, are used to calculate specific examples illustrating effects produced by such factors as aspect ratio, thickness ratio, taper ratio, sweep angle, airspeed, altitude, material density, and stiffness.

Because of the simplifications involved in the analysis, the results are to be considered chiefly qualitative in nature and are intended to be of use primarily in selecting practical wings for research programs or in other instances where the weighing of aeroelastic effects in the determination of practical ranges for wing parameters is desirable. Quantitative evaluation of the effects of changes in wing geometry, however, are believed to be provided by the results and absolute values of the aeroelastic characteristics of a wing may be obtained if the aeroelastic characteristics of a related practical wing are known and this wing is used as a basis for comparison.

SYMBOLS

a_s area of solid airfoil section measured perpendicular to elastic axis, sq ft

a_o nondimensional area of solid airfoil section measured perpendicular to elastic axis, $a_s/T'(c')^2$

a cross-sectional area of skin of assumed hollow airfoil section measured perpendicular to elastic axis, $2a_oT'r(c')^2$, sq ft

$\bar{a}$ area enclosed by mean line of skin of airfoil section measured perpendicular to elastic axis, sq ft

A aspect ratio, $(2s)^2/S$

c chord of swept wing in direction of free stream, ft

c' chord of transformed wing perpendicular to elastic axis, $c \cos \gamma$, ft

$\bar{c}$ mean aerodynamic chord of swept wing in direction of free stream, ft

C_L wing lift coefficient, L/qS

ΔC_L incremental lift coefficient due to wing bending, $\Delta L/qS$

ΔC_m incremental pitching-moment coefficient about aerodynamic center of rigid wing due to wing bending, $\Delta M/qS\bar{c}$

d streamwise distance from aerodynamic center of a given spanwise section to aerodynamic center of rigid wing, ft

e distance from center of pressure of airfoil section to elastic axis, percent of chord

E Young's modulus of elasticity of wing structural material, lb/sq ft

g gravitational acceleration, ft/sec^2

G torsional modulus of rigidity of wing structural material, lb/sq ft

I_S bending moment of inertia of solid airfoil section measured perpendicular to elastic axis, ft^4

I_O nondimensional moment of inertia of solid airfoil section measured perpendicular to elastic axis, $I_S/(T')^3(c')^4$

I moment of inertia of assumed hollow airfoil section measured perpendicular to elastic axis, $I_O(T')^3(c')^4\left[1 - (1 - 2r)^3\right]$, ft^4

J torsional moment of inertia of hollow airfoil section measured perpendicular to elastic axis, ft^4

k chordwise location on transformed wing of front shear web from leading edge and of rear shear web from trailing edge, fraction of chord

K proportionality constant related to spanwise distribution of loading over wing

l tail length, streamwise distance between point for neutral static stability with respect to angle of attack and center of pressure of horizontal tail, ft

L wing lift, lb

ΔL incremental lift due to wing bending, lb

M moment, ft-lb

ΔM incremental pitching moment, produced about aerodynamic center of rigid wing, due to wing bending, ft-lb

n normal acceleration, g units

p magnitude of uniformly distributed load, lb/sq ft

q dynamic pressure, $\rho V^2/2$, lb/sq ft

r ratio of wing-skin thickness to airfoil-section thickness (assumed constant along chord)

s semispan of swept wing, ft

s' semispan of transformed wing, $s/\cos\gamma$, ft

S wing area, sq ft

S_t — tail area, sq ft

t — airfoil skin thickness, ft

T — ratio of airfoil-section maximum thickness to chord measured in direction of free stream

T' — ratio of airfoil-section maximum thickness to chord measured perpendicular to elastic axis, $T/\cos \gamma$

V — airspeed, ft/sec

w — weight density of wing structural material, lb/cu ft

W_G — airplane gross weight, lb

W — wing structural weight, lb

W_W — wing total weight, lb

x' — chordwise station on transformed wing measured from leading edge, positive forward, ft

$\bar{x}$ — streamwise location of aerodynamic center measured from leading edge of mean aerodynamic chord, positive forward, ft

$\Delta\bar{x}$ — shift in wing aerodynamic-center location due to wing bending, positive forward, ft

x_n — streamwise location of center-of-gravity position for neutral static stability with respect to angle of attack measured from leading edge of mean aerodynamic chord, positive forward, ft

$\left(x_{cp}\right)_{\Delta L}$ — center of pressure of loss in lift due to wing bending, measured from leading edge of mean aerodynamic chord, positive forward, ft

y — spanwise station on swept wing (see fig. 1), ft

y' — spanwise station on transformed wing (see fig. 1) $y/\cos \gamma$, ft

$\bar{y}$ — spanwise location of mean aerodynamic chord of swept wing (see fig. 1), ft

α angle of attack, radians

$\Delta\alpha$ change in local angle of attack due to aeroelastic
                      distortion, radians

γ angle of sweep of elastic axis, deg

θ local torsional deflection of chord of transformed wing
                      relative to root chord, radians

λ plan-form taper ratio, ratio of tip chord to root chord

Λ angle of sweep of axis which is assumed to contain aerodynamic
                      centers of all sections along span, deg

ξ floating spanwise coordinate on transformed wing
                      (see fig. 1), ft

ρ air density, slugs/cu ft

σ wing stress in extreme fiber, lb/sq ft

τ taper ratio of thickness ratio, T_{tip}/T_{root}

dz'/dy' slope of elastic axis measured in plane perpendicular
                      to chord plane of wing

$d\epsilon/d\alpha$ variation of average angle of downwash at tail with angle
                      of attack, per radian

C_{L_α} variation of lift coefficient with angle of attack,
                      per radian

$\left(C_{L_\alpha}\right)_B$ variation of lift coefficient with angle of attack
                      associated with angle-of-attack changes due to wing
                      bending, per radian

$f_1(\lambda,\tau)$ function of taper ratio related to incremental lift
                      parameter

$f_2(\lambda,\tau)$ function of taper ratio related to incremental moment parameter

$f_3(\lambda)$ function of taper ratio defined by $\dfrac{4}{3}\dfrac{1 + \lambda + \lambda^2}{(1 + \lambda)^2}$

Subscripts:

y	spanwise station y
y'	spanwise station y'
ξ	spanwise coordinate ξ
r	wing root
wb	wing-body combination
w	wing
t	tail
B	bending
T	torsion
R	rigid wing
F	flexible wing
i	inertia
a	aerodynamic
av	average
1	first extreme loading condition (see appendix)
2	second extreme loading condition (see appendix)

ASSUMPTIONS AND LIMITATIONS OF ANALYSIS

Because application of refined methods of aeroelastic analysis
would be extremely laborious when applied to the determination of the
effects of wide variations in wing external geometry, the method out-
lined herein for analysis of the effect of wing distortion on longi-
tudinal stability involves simplifying assumptions and limitations.
Although these simplifications prevent the attainment of precise quan-
titative conclusions, the objective of qualitatively indicating prac-
tical ranges for various design parameters is believed to be attained.
Further justification for the simplifications derives from the fact
that many of the parameters necessary for a more refined analysis have

not been and possibly cannot be accurately determined in the transonic speed range.

The present analysis applies to shell-wing structures (that is, the load is taken primarily in the skin) in which the chordwise variation of skin thickness is proportional to the local airfoil-section thickness, and the spanwise variation in skin thickness is of a character to give a constant spanwise stress in the extreme fiber under a uniformly distributed loading. This structure was chosen for ease in computation and, although not a typical practical case, represents an efficient structure because the structural material is concentrated far from the elastic axis. The airfoil shape is arbitrary.

Initially, in the present analysis, the effects of wing bending alone are considered and, in general, the results which are presented were obtained for this case. The effects of torsion are included by subsequent calculations of the ratio of angle-of-attack changes resulting from torsion to those resulting from bending; these ratios can be used to apply corrections to the results obtained through consideration of bending alone. The effects of the camber produced by both torsion and bending were neglected as these effects are relatively small.

Inertia loadings are not considered in the analytical development and, therefore, the results apply only to airplanes which have a large percentage of their gross weight concentrated near the midspan. The alleviating effects of wing weight are considered briefly in the section entitled "Results and Discussion."

In order to compute bending deflections under a given load (or stress), the swept wings were transformed to unswept wings as shown in figure 1. This transformation is not exact for the case of wings having tapered plan forms; however, the error is small except for combinations of low plan-form taper ratio and low aspect ratio. The root restraint for the transformed wing does not represent exactly the conditions for an actual swept wing because a streamwise twist due to bending which occurs near the root of a swept wing does not occur for the transformed wing. An analysis based on the assumed root restraint is believed adequate for the following reasons:

(1) For many combinations of aspect ratio and sweep, the root twist is small compared to the angle-of-attack changes due to bending.

(2) There is a wide variation in the root-restraint conditions in actual airplane designs.

(3) Some experimental evidence exists which indicates that the bending deflections obtained for the transformed wing closely approximate

those for the swept wing when the effective root is chosen in the manner used herein.

Inasmuch as a direct algebraic solution for the aeroelastic effects considered herein was desired, it was necessary to express the spanwise load distribution responsible for the distortion in algebraic form. The feasibility of such a procedure was therefore investigated, and the results are presented in the appendix. These results indicate that the bending distortion of a wing supporting a given total load is fairly insensitive to the assumed form of the spanwise loading; in fact, the load shapes which result in approximately the same distortion are sufficiently broad to encompass the loadings to be expected on wings operating at widely differing flight conditions and having widely differing geometric parameters such as aspect ratio, sweepback angle, and taper ratio, as well as fairly large differences in degree of flexibility.

On the basis of the results presented in the appendix, use of a representative average type of spanwise load distribution for purposes of computing the angle-of-attack changes resulting from bending deflections appears to have at least limited application. The appendix also indicates that a uniformly distributed aerodynamic loading meets the requirements of a representative average type, and a uniform load modified by a tip correction was assumed for use in computing the angle-of-attack changes. Since the procedure used herein for examining aeroelastic effects primarily requires a knowledge of the difference between the loading on the rigid and flexible wings and since this difference was determined directly from the angle-of-attack changes due to the bending deflections, the exact details of the absolute loadings on either the rigid or flexible wing were not considered. The magnitude of the assumed uniform loading was determined by the operating lift coefficient of the distorted wing. This approach differs from the first step in the usual iterative or relaxation procedures (see ref. 2, for example), wherein the load on the undistorted wing is used to compute an initial estimation of the distortion. The present approach affords a more accurate estimation of the distortion than is obtained from this first iterative step in that the magnitude of the loading assumed is correct and only its distribution is somewhat arbitrary. The angle-of-attack changes associated with the assumed loading were used to establish the difference in load between the rigid and flexible wings at any given section by assuming that this difference was proportional to the product of the change in local angle of attack and the lift-curve slope of the rigid wing.

METHOD OF ANALYSIS

Effects of wing bending.- The method of analysis involves relating the wing stress per g normal acceleration, the loss in wing lift due to bending, and/or the wing aerodynamic-center shift due to bending to the wing structural weight (these relations being a function of the wing

external geometry, structural material, and the flight condition). For the transformed wing (see fig. 1), the stress at any spanwise station is approximated by the usual formula:

$$\sigma = \frac{M_B T' c'}{2I} \tag{1}$$

where

$$c' = c'_r\left[1 - (1 - \lambda)\frac{y'}{s'}\right]$$

$$T' = T'_r\left[1 - (1 - \tau)\frac{y'}{s'}\right]$$

$$I = I_0(T')^3(c')^4(6r - 12r^2 + 8r^3)$$

$$M_B = \int_{y'}^{s'} pc'_\xi(\xi - y')\, d\xi$$

$$c'_\xi = c'_r\left[1 - (1 - \lambda)\frac{\xi}{s'}\right]$$

As may be seen from the foregoing expression for thickness ratio, taper in thickness ratio was assumed to have a linear variation along the span.

Performance of the indicated substitutions in equation (1) together with the following relations

$$\frac{s'}{c'_r T'_r} = \frac{A(1 + \lambda)}{4T_r \cos \gamma}$$

$$T_r = \frac{2T_{av}}{1 + \tau}$$

$$p = \frac{W_G n}{S}$$

results in an expression which relates the wing stress and loading to nondimensional geometric parameters of the wing

$$\frac{W_G/S}{\sigma/n}\frac{1}{I_0}\left(\frac{A}{T_{av}\cos\gamma}\right)^2 =$$

$$\frac{128}{(1 + \tau)^2(1 + \lambda)^2}\frac{\left[1 - (1 - \lambda)\frac{y}{s}\right]^3\left(6r - 12r^2 + 8r^3\right)\left[1 - (1 - \tau)\frac{y}{s}\right]^2}{\frac{1 + 2\lambda}{6} - \frac{1 + \lambda}{2}\frac{y}{s} + \frac{1}{2}\left(\frac{y}{s}\right)^2 - \frac{1 - \lambda}{6}\left(\frac{y}{s}\right)^3} \tag{2}$$

For a given value of the left-hand member, hereinafter referred to as
the "stress parameter," and for given taper ratios, equation (2) deter-
mines the spanwise variation of the ratio of skin thickness to local
airfoil-section thickness. Typical variations of a parameter propor-
tional to skin thickness are presented in figure 2 for various plan-
form and thickness taper ratios. The comparison applies to wings having
the same area, sweep, aspect ratio, and average section thickness and
having the same extreme-fiber stress under a given uniform loading.
When the variation of skin thickness along the span is known, the wing
structural weight for a given structural material can be determined from
the relation

$$W = 2w \int_0^{s'} a \, dy' \qquad (3)$$

where

$$a = 2a_0 T'(c')^2 r$$

Performance of the indicated substitution in equation (3) together
with the following relation

$$s'(c'_r)^2 T'_r = \frac{2T_r}{(1 + \lambda)^2} \sqrt{\frac{s^3}{A}}$$

results in an expression for wing structural weight as a function of the
variation of skin thickness along the span

$$\frac{WA^{1/2}}{s^{3/2} wa_0 T_{av}} = \frac{16}{(1 + \tau)(1 + \lambda)^2} \int_0^{1.0} r \left[1 - (1 - \lambda)\frac{y}{s}\right]^2 \left[1 - (1 - \tau)\frac{y}{s}\right] d \frac{y}{s}$$

$$(4)$$

The left-hand member of equation (4) is hereinafter referred to as the
"weight parameter." Variations along the span of a parameter propor-
tional to incremental wing weight are shown in figure 3 for various plan-
form and thickness taper ratios. These wing-weight variations corre-
spond to the skin-thickness variations of figure 2.

Equations (2) and (4) can be combined graphically so that an evalua-
tion of the weight parameter as a function of the stress parameter for

various values of the taper ratios λ and τ can be made. This relationship may be expressed as

$$\frac{W}{S^{3/2}} \frac{A^{1/2}}{w a_0 \tau_{av}} = f\left[\frac{W_G/S}{\sigma/n} \frac{1}{I_0}\left(\frac{A}{\tau_{av} \cos \gamma}\right)^2, \lambda, \tau\right] \tag{5}$$

The relationship between these two parameters is shown in figure 4 for various values of the taper ratios λ and τ.

For the assumed wing structure and within the limitations of this analysis, the curves of figure 4 can be used to determine the wing structural weight for a given stress per g normal acceleration provided the wing structural material, wing external geometry, and the airplane wing loading are known. Conversely, if the wing structural weight is specified, the corresponding stress per g normal acceleration may be determined.

The stress parameter can easily be converted to parametric expressions for the aeroelastic effects considered herein. The ratio $\dfrac{W_G/S}{\sigma/n}$ which appears in the stress parameter (see eq. 2) can be written in terms of the loss in wing lift or the wing aerodynamic-center shift due to bending by evaluating the angle-of-attack changes along the span resulting from the bending and then integrating the incremental loss in lift at each section and the associated incremental pitching moments that are thus produced about the aerodynamic center of the rigid wing.

As stated in the foregoing development, the spanwise variations in skin thickness and wing structural weight were chosen so that a constant spanwise stress would occur in the extreme fiber under a uniformly distributed load. With this type of skin-thickness distribution the stress along the span under an actual loading would be expected to be reasonably constant except in the vicinity of the tip where a gradual decrease in stress would occur due in part to the usual decrease in loading as the tip is approached. In addition, the stipulation of a constant stress out to the tip under any loading dictates that the skin thickness go to zero at the tip. At least a small finite skin thickness would exist at the tip for the practical case and, although such a modification would not significantly affect the wing structural weight calculated by the preceding method, it would result in a decrease in stress to zero as the wing tip is approached. In order to account for these factors in the computations of the change in angle of attack due to wing bending, the wing stress was assumed constant to 0.8 semispan but was assumed to have a linear variation from 0.8 semispan to zero at the tip.

When these assumptions are applied, the angle-of-attack change along the span may be obtained from the following relations:

$$\Delta\alpha_B = - \frac{dz'}{dy'} \sin\gamma \qquad (6)$$

and

$$\frac{dz'}{dy'} = \int_0^{y'} \frac{2\sigma_{y'}}{ET'c'} \, dy' = \frac{2s'}{E} \int_0^{y'/s'} \frac{\sigma_{y'}}{c'T'} \, d\frac{y'}{s'}$$

For $\quad 0 < \dfrac{y'}{s'} < 0.8$,

$$\sigma_{y'} = \sigma$$

and

$$\frac{dz'}{dy'} = \frac{2\sigma s'}{ET'_r c'_r} \int_0^{y'/s'} \frac{1}{\left[1 - (1-\tau)\frac{y'}{s'}\right]\left[1 - (1-\lambda)\frac{y'}{s'}\right]} \, d\frac{y'}{s'}$$

Integration of the preceding expression, substitution into equation (6), and subsequent rearrangement of the results yields

$$\frac{\Delta\alpha_B ET_{av}}{\sigma A \tan\gamma} = \frac{1+\tau}{4} \frac{1+\lambda}{\tau-\lambda} \left\{ \log_e\left[1 - (1-\lambda)\frac{y}{s}\right] - \log_e\left[1 - (1-\tau)\frac{y}{s}\right] \right\} \qquad (7a)$$

For $\quad 0.8 < \dfrac{y'}{s'} < 1.0$,

$$\sigma_{y'} = 5\sigma\left(1 - \frac{y'}{s'}\right)$$

and

$$\frac{dz'}{dy'} = \frac{2\sigma s'}{ET'_r c'_r} \left\{ \int_0^{0.8} \frac{1}{\left[1 - (1 - \tau)\frac{y'}{s'}\right]\left[1 - (1 - \lambda)\frac{y'}{s'}\right]} \, d\frac{y'}{s'} + \right.$$

$$5 \int_{0.8}^{y'/s'} \frac{1}{\left[1 - (1 - \tau)\frac{y'}{s'}\right]\left[1 - (1 - \lambda)\frac{y'}{s'}\right]} \, d\frac{y'}{s'} -$$

$$\left. 5 \int_{0.8}^{y'/s'} \frac{y'/s'}{\left[1 - (1 - \tau)\frac{y'}{s'}\right]\left[1 - (1 - \lambda)\frac{y'}{s'}\right]} \, d\frac{y'}{s'} \right\}$$

Integration of the preceding expression, then substitution into equation (6), and subsequent rearrangement gives

$$\frac{\Delta\alpha_B ET_{av}}{\sigma A \tan \gamma} = \frac{1 + \tau}{4} \frac{1 + \lambda}{\tau - \lambda} \left\{ \left(4 + \frac{5}{\tau - 1}\right) \log\left[1 - 0.8(1 - \tau)\right] - \right.$$

$$\left(4 + \frac{5}{\lambda - 1}\right) \log\left[1 - 0.8(1 - \lambda)\right] + \left(5 + \frac{5}{\lambda - 1}\right) \log\left[1 - \right.$$

$$\left. (1 - \lambda)\frac{y}{s}\right] - \left(5 + \frac{5}{\tau - 1}\right) \log\left[1 - (1 - \tau)\frac{y}{s}\right] \right\} \qquad (7b)$$

The parameter $\dfrac{\Delta\alpha_B ET_{av}}{\sigma A \tan \gamma}$ is plotted in figure 5 for various plan-form and thickness taper ratios. This parameter gives the variation along the span of the change in angle of attack produced by wing bending. A point worth noting is that the comparison of plan-form and thickness taper ratios shown in figure 5 is for wings having the same stress rather than the same structural weight. On this basis, the wings

become progressively lighter as the plan-form or the thickness taper ratio is decreased.

The incremental lift associated with the angle-of-attack changes due to bending may be written in the following form:

$$\Delta L = 2qs \int_0^{1.0} \left(C_{L_\alpha}\right)_B \Delta\alpha_B c \ d \ \frac{y}{s}$$

The lift-curve slope $\left(C_{L_\alpha}\right)_B$ associated with angle-of-attack changes due to bending is assumed to be the same as the lift-curve slope for the rigid wing in the region $0 < \frac{y}{s} < 0.8$ but has a parabolic variation to zero at the tip in the region $0.8 < \frac{y}{s} < 1.0$ in order to account for the usual decrease in lift as the tip is approached.

For $0 < \frac{y}{s} < 0.8$,

$$\left(C_{L_\alpha}\right)_B = \left(C_{L_\alpha}\right)_R$$

For $0.8 < \frac{y}{s} < 1.0$,

$$\left(C_{L_\alpha}\right)_B = 5\left(C_{L_\alpha}\right)_R \left[8 \ \frac{y}{s} - 5\left(\frac{y}{s}\right)^2 - 3\right]$$

When this assumption and the previously developed expressions for $\Delta\alpha_B$ and c are used, the incremental load takes the following form:

$$\Delta L = \frac{qs}{2}\left(C_{L\alpha}\right)_R \frac{c_r \sigma A \tan \gamma}{ET_{av}} \frac{(1 + \tau)(1 + \lambda)}{\tau - \lambda} \left(\int_0^{0.8} \left[1 - \right.\right.$$

$$(1 - \lambda)\frac{y}{s}\right] \left\{\log\left[1 - (1 - \lambda)\frac{y}{s}\right] - \log\left[1 - (1 - \tau)\frac{y}{s}\right]\right\} d\frac{y}{s} +$$

$$5\int_{0.8}^{1.0} \left[1 - (1 - \lambda)\frac{y}{s}\right] \left[8\frac{y}{s} - 5\left(\frac{y}{s}\right)^2 - 3\right] \left\{\left(4 + \frac{5}{\tau - 1}\right)\log\left[1 - \right.\right.$$

$$0.8(1 - \tau)\right] - \left(4 + \frac{5}{\lambda - 1}\right)\log\left[1 - 0.8(1 - \lambda)\right] +$$

$$\left(5 + \frac{5}{\lambda - 1}\right)\log\left[1 - (1 - \lambda)\frac{y}{s}\right] -$$

$$\left(5 + \frac{5}{\tau - 1}\right)\log\left[1 - (1 - \tau)\frac{y}{s}\right]\right\} d\frac{y}{s}\right) \tag{8}$$

The incremental lift may be expressed in coefficient form and in terms of the nondimensional geometric parameters of the wing through use of the following relations:

$$\frac{\Delta L}{L} = \frac{\Delta L}{pS} = \frac{\Delta C_L}{C_L}$$

and

$$\frac{sc_r}{S} = \frac{1}{1 + \lambda}$$

The substitution of these relationships into equation (8) and subsequent rearrangement gives

$$\frac{\Delta C_L}{C_L} \frac{p}{\sigma} \frac{ET_{av}}{qA} \frac{1}{\left(C_{L_\alpha}\right)_R \tan \gamma} = \int_0^{0.8} \frac{1 + \tau}{2} \frac{1}{\tau - \lambda}\left[1 - (1 - \lambda)\frac{y}{s}\right]\left\{\log\left[1 - \right.\right.$$

$$\left.(1 - \lambda)\frac{y}{s}\right] - \log\left[1 - (1 - \tau)\frac{y}{s}\right]\right\} d\frac{y}{s} + \int_{0.8}^{1.0} \frac{5}{2}\frac{1 + \tau}{\tau - \lambda}\left[1 - (1 - \lambda)\frac{y}{s}\right]\left[8\frac{y}{s} - \right.$$

$$5\left(\frac{y}{s}\right)^2 - 3\right]\left\{\left(4 + \frac{5}{\tau - 1}\right)\log\left[1 - 0.8(1 - \tau)\right] - \left(4 + \frac{5}{\lambda - 1}\right)\log\left[1 - \right.\right.$$

$$\left.0.8(1 - \lambda)\right] + \left(5 + \frac{5}{\lambda - 1}\right)\log\left[1 - (1 - \lambda)\frac{y}{s}\right] - $$

$$\left(5 + \frac{5}{\tau - 1}\right)\log\left[1 - (1 - \tau)\frac{y}{s}\right]\right\} d\frac{y}{s} \qquad (9)$$

The expressions within the integrals on the right-hand side of equation (9) are proportional to the variation along the span of the change in lift due to wing bending. Typical spanwise variations of the change in lift produced by wing bending are plotted in figure 6 for various plan-form and thickness taper ratios. Note again that the comparison of taper ratios is for wings having the same stress rather than the same structural weight. The sum of the integrals on the right-hand side of equation (9), which is used herein in determining the change in lift, is defined as $f_1(\lambda, \tau)$. The values of this function are plotted against plan-form taper ratio in figure 7 for $\tau = 1.0$ and $\tau = 0.5$.

Solution of equation (9) for the ratio of average loading to stress yields

$$\frac{p}{\sigma} = \frac{W_G/S}{\sigma/n} = \frac{\left(C_{L_\alpha}\right)_R f_1(\lambda,\tau) \tan \gamma}{\Delta C_L / C_L} \frac{qA}{ET_{av}}$$

Substitution of this expression into equation (5) relates a parameter, defined herein as the "incremental lift parameter," to the weight parameter, that is,

$$\frac{W}{S^{3/2}} \frac{A^{1/2}}{wa_0 T_{av}} = f\left[\frac{1}{\Delta C_L / C_L} \frac{q}{EI_0}\left(\frac{A}{T_{av}}\right)^3 \left(C_{L_\alpha}\right)_R \frac{\tan \gamma}{\cos^2 \gamma} f_1(\lambda,\tau),\lambda,\tau\right] \quad (10)$$

This expression is in the same form as the relation between the stress parameter and the weight parameter. Therefore, the incremental lift parameter may also be considered the abscissa of the plots shown in figure 4. Within the limitations of the analysis, the curves of figure 4 therefore can be used to determine the wing structural weight for a given loss in lift due to wing bending and vice versa.

The lift-curve slope of the flexible wing may be expressed in terms of $\Delta C_L / C_L$ (see eq. 9) and the lift-curve slope of the rigid wing. For the flexible wing

$$L_F = \left(C_{L_\alpha}\right)_F \alpha q S$$

For the flexible wing the lift equals the lift of the rigid wing plus the change in lift due to bending (negative for sweptback wings at positive angle of attack)

$$L_F = L_R + \Delta L = \left(C_{L_\alpha}\right)_R \alpha q S + \Delta L$$

The preceding two equations can be combined and rearranged to give

$$\frac{\left(C_{L_\alpha}\right)_F}{\left(C_{L_\alpha}\right)_R} = \frac{L_F}{L_F - \Delta L} = \frac{1}{1 - \dfrac{\Delta C_L}{C_L}} \quad (11)$$

Note that $\Delta C_L / C_L$ in itself is a function of $\left(C_{L_\alpha}\right)_R$. (See eq. (10).)

The incremental pitching moment associated with the angle-of-attack changes due to bending may be written in the following form:

$$\Delta M = 2qs \int_0^{1.0} \left(C_{L_\alpha}\right)_B \Delta\alpha_B c d\, d\frac{y}{s} \tag{12}$$

where (see fig. 1)

$$d = \overline{y} \tan \Lambda - y \tan \Lambda$$

In spanwise coordinates

$$\frac{\overline{y}}{s} = \frac{1}{3} \frac{1 + 2\lambda}{1 + \lambda}$$

and

$$d = s\left(\frac{1}{3} \frac{1 + 2\lambda}{1 + \lambda} - \frac{y}{s}\right) \tan \Lambda$$

When this expression for d and the expressions previously presented for $\Delta\alpha_B$, $\left(C_{L_\alpha}\right)_B$, and c are substituted into the pitching-moment equation (eq. 12), the form of the equation is

$$\Delta M = \frac{qs^2}{2}\left(C_{L_\alpha}\right)_R \frac{c_r \alpha A \tan \gamma}{E\tau_{av}} \tan \Lambda \frac{(1 + \tau)(1 + \lambda)}{\tau - \lambda} \left(\int_0^{0.8} \left[\frac{1}{3} \frac{1 + 2\lambda}{1 + \lambda} - \frac{y}{s}\right]\left[1 - (1 - \lambda)\frac{y}{s}\right]\left\{\log\left[1 - (1 - \lambda)\frac{y}{s}\right] - \right.\right.$$

$$\log\left[1 - (1 - \tau)\frac{y}{s}\right]\right\} d\frac{y}{s} + 5\int_{0.8}^{1.0} \left(\frac{1}{3}\frac{1 + 2\lambda}{1 + \lambda} - \frac{y}{s}\right)\left[1 - (1 - \lambda)\frac{y}{s}\right]\left[8\frac{y}{s} - 5\left(\frac{y}{s}\right)^2 - 3\right]\left\{\left(4 + \right.\right.$$

$$\left.\frac{5}{\tau - 1}\right) \log\left[1 - 0.8(1 - \tau)\right] - \left(4 + \frac{5}{\lambda - 1}\right)\log\left[1 - 0.8(1 - \lambda)\right] + \left(5 - \frac{5}{\tau - 1}\right)\log\left[1 - (1 - \lambda)\frac{y}{s}\right] - $$

$$\left(5 + \frac{5}{\tau - 1}\right)\log\left[1 - (1 - \tau)\frac{y}{s}\right]\right\} d\frac{y}{s}\right) \tag{13}$$

In order to express equation (13) in coefficient form and in terms of nondimensional geometric parameters of the wing, the following relations are used:

$$\frac{\Delta M}{L} = \frac{\Delta M}{pS} = \frac{\Delta C_m q S \bar{c}}{C_L q S} = \frac{\Delta C_m \bar{c}}{C_L}$$

$$\frac{s^2}{S} \frac{c_r}{\bar{c}} = \frac{3}{8} A \frac{1 + \lambda}{1 + \lambda + \lambda^2}$$

When these relationships are substituted into equation (13) and the resulting equation is rearranged, the following expression is obtained:

$$\frac{\Delta C_m}{C_L} \frac{p}{\sigma} \frac{E}{q} \frac{T_{av}}{A^2} \frac{1}{\left(C_{L\alpha}\right)_R \tan \gamma \tan \Lambda} = \int_0^{0.8} \frac{3}{16} \frac{(1 + \lambda)^2}{1 + \lambda + \lambda^2} \frac{1 + \tau}{\tau - \lambda} \left(\frac{1}{3} \frac{1 + 2\lambda}{1 + \lambda} - \right.$$

$$\left. \frac{y}{s}\right)\left[1 - (1 - \lambda)\frac{y}{s}\right] \left\{ \log\left[1 - (1 - \lambda)\frac{y}{s}\right] - \log\left[1 - (1 - \tau)\frac{y}{s}\right]\right\} d\frac{y}{s} +$$

$$\int_{0.8}^{1.0} \frac{15}{16} \frac{(1 + \lambda)^2}{1 + \lambda + \lambda^2} \frac{1 + \tau}{\tau - \lambda} \left(\frac{1}{3} \frac{1 + 2\lambda}{1 + \lambda} - \frac{y}{s}\right)\left[1 - (1 - \lambda)\frac{y}{s}\right]\left[8 \frac{y}{s} - \right.$$

$$\left. 5\left(\frac{y}{s}\right)^2 - 3\right]\left\{\left(4 + \frac{5}{\tau - 1}\right) \log\left[1 - 0.8(1 - \tau)\right] - \left(4 + \frac{5}{\lambda - 1}\right) \log\left[1 - \right.\right.$$

$$0.8(1 - \lambda)\right] + \left(5 + \frac{5}{\lambda - 1}\right) \log\left[1 - (1 - \lambda)\frac{y}{s}\right] -$$

$$\left(5 + \frac{5}{\tau - 1}\right) \log\left[1 - (1 - \tau)\frac{y}{s}\right]\right\} d\frac{y}{s} \qquad (14)$$

The expressions within the integrals on the right-hand side of equation (14) are proportional to the variation along the span of the

incremental pitching moment due to wing bending. Typical spanwise
variations of the pitching moments produced by wing bending are plotted
in figure 8 for various plan-form and thickness taper ratios. The
effect of taper ratio shown applies to wings of constant stress. The
sum of the integrals on the right-hand side of equation (14), which is
used herein to determine the pitching moment produced by wing bending,
is defined as $f_2(\lambda,\tau)$. The values of this function are plotted in
figure 7 against plan-form taper ratio.

Solution of equation (14) for the ratio of incremental loading to
stress yields

$$\frac{p}{\sigma} = \frac{W_G/S}{\sigma/n} = \frac{\left(C_{L_\alpha}\right)_R \tan \gamma \tan \Lambda}{\Delta C_m/C_L} \frac{q}{E} \frac{A^2}{T_{av}} f_2(\lambda,\tau)$$

Substitution of this expression into equation (5) relates a parameter
defined herein as the "incremental moment parameter" to the weight
parameter; that is,

$$\frac{W}{S^{3/2}} \frac{A^{1/2}}{w a_0 T_{av}} = f\left[\frac{1}{\Delta C_m/C_L} \frac{q}{EI_0} \frac{A^4}{T_{av}^3}\left(C_{L_\alpha}\right)_R \frac{\tan \gamma \tan \Lambda \, f_2(\lambda,\tau)}{\cos^2 \gamma}, \lambda, \tau\right] \quad (15)$$

This expression is in the same form as the relation between the stress
and the weight parameter; therefore, the incremental moment parameter
may also be considered as the abscissa of the plots shown in figure 4.
The factor $\Delta C_m/C_L$ of the incremental moment parameter is the shift
in the aerodynamic center of the wing (expressed in chord lengths) due
to bending; that is,

$$\frac{\Delta C_m}{C_L} = \frac{\Delta \bar{x}}{\bar{c}}$$

Within the limitations of this analysis the curves of figure 4 therefore
can be used to determine the wing structural weight for a given allowable
aerodynamic-center shift and vice versa.

Because the aerodynamic-center shift in terms of actual distance
will vary with aspect ratio when the shift is expressed in chord lengths,
for some purposes a better comparison is afforded when the shift is

expressed in terms of $\sqrt{S}$ (based on over-all size of the airplane).
The relationship between $\Delta \bar{x}/\bar{c}$ and $\Delta \bar{x}/\sqrt{S}$ may be developed from the
expression

$$\bar{c} = \frac{4}{3} \frac{1 + \lambda + \lambda^2}{(1 + \lambda)^2} \sqrt{\frac{S}{A}}$$

so that

$$\frac{\Delta \bar{x}}{\sqrt{S}} = \frac{\Delta \bar{x}}{\bar{c}} \frac{1}{\sqrt{A}} \frac{4}{3} \frac{1 + \lambda + \lambda^2}{(1 + \lambda)^2}$$

The function $\dfrac{4}{3} \dfrac{1 + \lambda + \lambda^2}{(1 + \lambda)^2}$ is defined herein as $f_3(\lambda)$ and is plotted
against plan-form taper ratio in figure 7.

The location of the center of pressure of the change in load pro-
duced by wing bending is another parameter useful for the study of the
effects of wing bending on the longitudinal stability of a complete
airplane. The streamwise location of this center of pressure expressed
in chord lengths from the aerodynamic center of the rigid wing is
$\Delta C_m/\Delta C_L$ which from a combination of equations (9) and (14) can be
expressed as follows:

$$\frac{\Delta C_m}{\Delta C_L} = A \tan \Lambda \frac{f_2(\lambda,\tau)}{f_1(\lambda,\tau)}$$

The ratio $\dfrac{f_2(\lambda,\tau)}{f_1(\lambda,\tau)}$ is plotted in figure 7 as a function of plan-form

taper ratio for thickness taper ratios of 1.0 and 0.5. When the aero-
dynamic center of the rigid wing is assumed to be located at one-quarter
of its mean aerodynamic chord, the expression for the center of pressure
of the change in load is

$$\frac{(x_{cp})_{\Delta L}}{\bar{c}} = -0.25 + A \tan \Lambda \frac{f_2(\lambda,\tau)}{f_1(\lambda,\tau)} \qquad (16)$$

Effects of wing torsion.- The variation of the torsional deflection of a wing along its span may be expressed in the following form:

$$\frac{d\theta}{dy'} = \frac{M_T}{GJ} = \frac{M_T}{G\frac{J}{I}I} = \frac{M_T}{M_B}\frac{\sigma}{G}\frac{2}{T'c'}\frac{J}{I} \tag{17}$$

The twisting moment may be expressed as

$$M_T = \int_{y'}^{s'} p(c')^2 e\, dy'$$

$$= (c'_r)^2 \int_{y'}^{s'} pe\left[1 - (1 - \lambda)\frac{y'}{s'}\right]^2 dy' \tag{18}$$

When a constant loading and a constant value of e along the span are assumed, the integration of equation (18) yields

$$M_T = pe(c'_r)^2 s'\left[\frac{1 + \lambda + \lambda^2}{3} - \frac{y}{s} + (1 - \lambda)\left(\frac{y}{s}\right)^2 - \frac{(1 - \lambda)^2}{3}\left(\frac{y}{s}\right)^3\right] \tag{19}$$

For a constant loading condition the bending moment may be expressed as (see expression for M_B following eq. 1):

$$M_B = pc'_r(s')^2\left[\frac{1 + 2\lambda}{6} - \frac{1 + \lambda}{2}\frac{y}{s} + \frac{1}{2}\left(\frac{y}{s}\right)^2 - \frac{1 - \lambda}{6}\left(\frac{y}{s}\right)^3\right]. \tag{20}$$

Dividing equation (19) by equation (20) to obtain the ratio of the twisting moment to bending moment gives the following expression

$$\frac{M_T}{M_B} = \frac{ec'_r}{s'}\frac{\left[\frac{1 + \lambda + \lambda^2}{3} - \frac{y}{s} + (1 - \lambda)\left(\frac{y}{s}\right)^2 - \frac{(1 - \lambda)^2}{3}\left(\frac{y}{s}\right)^3\right]}{\left[\frac{1 + 2\lambda}{6} - \frac{1 + \lambda}{2}\frac{y}{s} + \frac{1}{2}\left(\frac{y}{s}\right)^2 - \frac{1 - \lambda}{6}\left(\frac{y}{s}\right)^3\right]} \tag{21}$$

In the analysis of the effects of torsion only wings with constant thickness ratio $(\tau = 1)$ are considered. When this assumption of constant thickness ratio is made, equation (21) is substituted into equation (17) and the result is rearranged and integrated, the torsional deflection may be expressed as

$$\frac{\theta TG \frac{J}{I} \cos \gamma}{2\sigma e} = \int_0^{y/s} \frac{\left[\frac{1 + \lambda + \lambda^2}{3} - \frac{y}{s} + (1 - \lambda)\left(\frac{y}{s}\right)^2 - \frac{(1 - \lambda)^2}{3}\left(\frac{y}{s}\right)^3\right]}{\left[1 - (1 - \lambda)\frac{y}{s}\right]\left[\frac{1 + 2\lambda}{6} - \frac{1 + \lambda}{2}\frac{y}{s} + \frac{1}{2}\left(\frac{y}{s}\right)^2 - \frac{1 - \lambda}{6}\left(\frac{y}{s}\right)^3\right]} \, d\frac{y}{s} \quad (22)$$

For the case of zero taper ratio, equation (22) simplifies to

$$\frac{\theta TG \frac{J}{I} \cos \gamma}{2\sigma e} = \int_0^{y/s} \frac{2}{1 - \frac{y}{s}} \, d\frac{y}{s}$$

$$= -2 \log_e\left(1 - \frac{y}{s}\right) \quad (23)$$

The torsional deflection is related to the angle of attack due to twist by

$$\theta = \frac{\Delta\alpha_T}{\cos \gamma} \quad (24)$$

Substituting equation (24) into equation (23) gives

$$\frac{\Delta\alpha_T TG \frac{J}{I}}{\sigma e} = -4 \log_e\left(1 - \frac{y}{s}\right) \quad (25)$$

The angle-of-attack change due to bending, $\Delta\alpha_B$ for $0 < \frac{y}{s} < 0.8$, is given by equation (7(a)). Substituting $\lambda = 0$ into equation (7(a)) gives the following equation:

$$\frac{\Delta\alpha_B ET}{\sigma A \tan \gamma} = \frac{1}{2} \log_e\left(1 - \frac{y}{s}\right) \quad (26)$$

Dividing equation (25) by equation (26) and solving for the ratio of angle-of-attack change due to torsion to the angle-of-attack change due to bending yields

$$\frac{\Delta\alpha_T}{\Delta\alpha_B} = - \frac{8Ee}{AG\,\frac{J}{I}\,\tan\gamma} \tag{27}$$

Similar computations for $\lambda = 1.0$ and $\tau = 1.0$ give

$$\frac{\Delta\alpha_T}{\Delta\alpha_B} = \frac{4\,\log_e\left(1 - \frac{y}{s}\right)Ee}{AG\,\frac{J}{I}\,\frac{y}{s}\,\tan\gamma} \tag{28}$$

RESULTS AND DISCUSSION

Comparison of effects of wing bending and wing torsion.- An examination of equations (27) and (28) shows that the ratio of the angle-of-attack changes due to torsion to those due to bending are inversely proportional to the aspect ratio and the tangent of the angle of sweepback. The over-all variation with sweepback would be approximately in inverse proportion to the angle of sweepback for small angles, but the angle-of-attack ratio would decrease rapidly at large angles of sweepback. These equations also indicate that the angle-of-attack change due to torsional deflections always opposes those due to bending whenever the center of pressure is ahead of the elastic axis. The angle-of-attack ratio for a plan-form taper ratio of zero is constant along the span; whereas for a taper ratio of unity the ratio has a variation along the span from a value one-half that for zero taper ratio at mid-span to infinity at the tip. The presence of this value of infinity at the tip results from the fact that the stress was assumed to remain constant out to the tip when the torsional deflections were considered. (See eq. 23.) As was pointed out previously in the practical case the bending stress would decrease near the tip to zero at the tip. Because of this consideration, the use of equation (28) should be limited to regions inboard of the 0.8 semispan as was done when bending deflection alone was considered. At the 0.8-semispan station the value of the ratio of change in angle of attack would be approximately the same for the unit taper ratio as for zero taper ratio.

In order to examine the actual ratios of angle-of-attack changes due to bending and torsion, it is necessary to know the values of the

ratios G/E and J/I. The ratio G/E is about the same for both steel and duralumin and has a value of about 0.37. The ratio J/I may have rather large variations and still maintain adequate strength in the wing. In fact, it is theoretically possible to adjust the torsional moment of inertia of a wing to obtain complete compensation of aeroelastic effects at a given flight condition (isoclinicism). In most cases, however, the torsional moment of inertia is dictated by other considerations such as those of flutter or control effectiveness.

In order to investigate the ratio of J/I inherent in an airfoil section having the type of structure assumed in the present report, the torsional moment of inertia of a symmetric parabolic-arc section was calculated from the relation

$$J = \frac{4(\bar{a})^2}{\oint \frac{ds}{t}} \tag{29}$$

where $\oint \frac{ds}{t}$ is a line integral taken around the mean periphery of the

torsion box consisting of the upper and lower skins and the shear webs.

The contribution of the areas forward of the front shear web and back of the rear shear web to $\bar{a}$ was neglected because it was relatively small and the contribution of the shear webs to the line integral (thin airfoil sections) was also neglected. For these conditions equation (29) may be written for a symmetric parabolic-arc section as follows:

$$J = \frac{4(\bar{a})^2}{2\oint_k^{c'-k} \frac{dx'}{rf(x')}} = \frac{2(\bar{a})^2 r}{c'\oint_{k/c'}^{1-\frac{k}{c'}} \frac{d\frac{x'}{c'}}{f(x')}} \tag{30}$$

where

$$f(x') = 4T'c' \frac{x'}{c'}\left(1 - \frac{x'}{c'}\right)$$

$$\bar{a} = c'(1 - r) \int_{k/c'}^{1 - \frac{k}{c'}} f(x') \, d\frac{x'}{s'}$$

$$= \frac{2}{3} T'(1 - r)(c')^2 \left[1 - 6\left(\frac{k}{c'}\right)^2 + 4\left(\frac{k}{c'}\right)^3 \right]$$

$$\oint_{k/c'}^{1 - \frac{k}{c'}} \frac{d\frac{x'}{c'}}{f(x')} = \frac{1}{2T'c'} \log_e \frac{1 - \frac{k}{c'}}{\frac{k}{c'}}$$

When the indicated substitutions into equation (30) are made and k is assumed to be equal to 0.2 (shear webs located at 20- and 80-percent chord), the value of the torsional moment of inertia becomes

$$J = 0.803(T')^3(c')^4(r - 2r^2 + r^3) \qquad (31)$$

Using the expression for I previously presented (see expression following eq. 1) and substituting for I_0 its value for a symmetric parabolic-arc section (0.0386) results in the following expression for the ratio J/I

$$\frac{J}{I} = 3.52 \frac{1 - 2r + r^2}{1 - 2r + \frac{4}{3} r^2} \qquad (32)$$

This ratio has some variation with skin-thickness ratio but the variation is slight except when the section approaches solidity; the value of J/I for the assumed section is about 3.5. This value is reasonably typical of values existing for actual wing sections.

When the value of J/I (3.5) and the value of G/E previously discussed (0.37) are used, equations (27) and (28) may be written

for $\lambda = 0$,

$$\frac{\Delta\alpha_T}{\Delta\alpha_B} = -\frac{6.2e}{A\,\tan\gamma} \tag{33}$$

and for $\lambda = 1.0$,

$$\frac{\Delta\alpha_T}{\Delta\alpha_B} = \frac{3.1\,\log_e\left(1 - \frac{y}{s}\right)}{y/s}\,\frac{e}{A\,\tan\gamma} \tag{34}$$

The values of e for a sweptback wing are not constant along the span, but the average value probably ranges from a maximum positive value of about 0.25 at subsonic speeds to small positive or negative values at supersonic speeds. By assuming a conservative value for e of 0.25, the ratio of angle of attack due to torsion to that due to bending has been plotted in figure 9 as a function of taper ratio and sweep angle. This figure shows that, for an angle of sweepback of the elastic axis of 45° and an aspect ratio of 4, the ratio of angle-of-attack change due to torsion to that due to bending would be about -0.38 for the zero-taper-ratio case. Reducing the aspect ratio to 2 results in this value being doubled and reducing the sweepback angle to 22.5° has a somewhat greater effect. Conversely, doubling the aspect ratio to 8 would halve this value, whereas increasing the sweepback angle would reduce this value much more rapidly. As mentioned previously, the values of the ratio for the constant-chord case are one-half the value for the zero-taper-ratio case at the root and about the same at the 0.8-semispan station. The variations presented in figure 9 indicate that, except for small sweepback angles (the order of 30°) or small aspect ratios (the order of 2) or particularly a combination of the two, the angle-of-attack changes produced by torsional deflections are appreciably less than those produced by bending deflections. In view of this result the remainder of this paper is concerned primarily with the effects of wing bending.

If the ratio of torsional moment of inertia to bending moment of inertia can be reduced from the value of 3.5 assumed in this analysis, the compensating effect of torsion would be increased. The distance between the aerodynamic center and the elastic axis also affects the amount of torsional compensation, and, in many cases, this distance will be less than the value of 0.25 chord used in the present analysis. A reduction in this value tends to reduce the compensating effect of torsion.

General effects of wing bending.- The effect of wing structural parameters, wing geometric parameters, and flight condition on the relation between the structural weight of a wing and aeroelastic effects dependent on wing bending stiffness may be examined through use of figure 4.

The structural-weight parameter, the ordinate of figure 4, indicates that the weight of a wing varies as the cube of a linear dimension (or as $S^{3/2}$). This variation is the type obtained with geometrically similar structures. The structural-weight variation with size for actual wings is found to be slightly less than the cubic relation because the efficiency of wing structures increase with increase in size, at least up to a certain point. These actual variations, however, are not reduced from the cubic variation a sufficient amount to prevent the weight of wings designed to a given stress from becoming prohibitive as their size is increased. The reason that the weight becomes prohibitive is that the lift-producing capabilities of a wing increase only as the square of a linear dimension. In order to circumvent this difficulty when the structural design of wings is dictated primarily by stress considerations, designers tend to reduce the allowable load factor as airplanes become larger; thus, the tendency for the weight to increase is retarded. When factors such as aerodynamic-center shift due to wing bending are a consideration, such an alternative is not afforded the designer because there is no reason to expect that the aerodynamic-center shift may be reduced significantly as the airplane size increases.

The stress parameter shown in figure 4 indicates that the allowable stress relative to the density of the structural material is a primary consideration in selection of the material when the wing structural design is dictated by strength alone. When stiffness governs a design, however, the incremental moment and lift parameters shown in figure 4 indicate that the modulus of elasticity of the structural material relative to its density also would be a primary consideration.

The incremental lift and moment parameters show that, as far as the effect of flight condition on aeroelastic effects is concerned, dynamic pressure is the primary variable. Mach number has only an indirect effect on aeroelastic phenomena. Changes in Mach number produce changes in the incremental lift or moment parameters through the effect of Mach number on the lift-curve slope of the wing. The relation between the lift-curve slope and the Mach number, aspect ratio, and sweep angle assumed for use in the examples presented herein is given by the expression

$$C_{L_\alpha} = \frac{2\pi}{\dfrac{\sqrt{1 - M^2\cos^2\Lambda}}{\cos\Lambda} + \dfrac{2}{A}}$$

where M is the Mach number. This expression is that given in reference 5 with the addition of the Prandtl-Glauert correction for compressibility which has been applied to the two-dimensional lift-curve slope. The formula gives values of lift-curve slope in reasonable agreement with those determined experimentally. A more rigorous determination of lift-curve slope from a simplified lifting-surface theory can be obtained through use of reference 6.

The stress, incremental lift, and incremental moment parameters reveal that the strength and stiffness characteristics of a wing are strongly affected by its external geometry. Increase in aspect ratio, sweep angle, or decrease in section thickness ratio caused rapid (high order) increases in stress and even more rapid increases in aeroelastic effects. In addition to the direct effects of aspect ratio on the parameters presented in figure 4, the lift-curve slope is affected by aspect ratio. The effect of an increase in aspect ratio on the wing lift-curve slope is in a direction to increase aeroelastic effects, and the effect of an increase in sweep angle on the wing lift-curve slope is in a direction to decrease aeroelastic effects. Although the area and moment of inertia of the airfoil section appears in the parameter presented in figure 4, the effects of the geometry of the airfoil section are generally small because of the limited variation of airfoil shapes which provide satisfactory aerodynamic characteristics. The variations in nondimensional moment of inertia I_0 of airfoil sections are larger than variations in nondimensional area a_0 but are much less significant than the effects of variations in the thickness ratio of these sections or the plan-form geometry of the wing.

Effects of wing external geometry.- In order to provide a better illustration of the manner in which various geometric properties of a wing affect its strength and its aeroelastic characteristics, the charts presented in figures 4 and 7 have been used to calculate the stress per g normal acceleration, the ratio between lift-curve slopes of the flexible and rigid wing, and the aerodynamic-center shift due to bending (in terms of both chord lengths and $\sqrt{S}$) for a series of duralumin wings flying at a Mach number of 0.9 at an altitude of 30,000 feet. All the wings have symmetric parabolic-arc sections, a structural weight typical of current practice $\left(W/S^{3/2} = 0.2\right)$, a plan-form taper ratio of 0.5, and no variation in section thickness ratio along the span. Wings for which the change in lift due to bending was greater than half the lift remaining on the distorted wing $\dfrac{\left(C_{L_\alpha}\right)_F}{\left(C_{L_\alpha}\right)_R} < \dfrac{2}{3}$ were not included in these calculations because limitations imposed by the assumptions used in the present analysis do not warrant such calculations. The preceding value was selected as a limit because a study indicated that, for the cases where losses in lift are larger than this value, the variation in load distribution from the assumed uniform type would, in some cases, be more extreme than the ones investigated in the appendix. As previously stated in "Assumptions and Limitations of Analyses" these investigated variations from the assumed load distribution have only a secondary effect on the predicted change in lift between the flexible and the rigid wing. When not limited by the foregoing restriction, calculations were made for aspect ratios up to 10 and sweep angles up to 65°.

The results of the calculations for this family of wings are summarized in figure 10 where the computed stress and aeroelastic parameters are plotted against sweepback angle for various aspect ratios and section thickness ratios. The stress per g is plotted in the form shown because the stress is determined by the magnitude of the loading $W_G n/S$ rather than by the acceleration alone. The effect of such variations is shown subsequently.

For wing structural weights typical of current practice, the variations shown in figure 10 indicate that for a very low thickness ratio (T = 0.04) only low aspect ratios (the order of 2) are usable for swept wings, and then both stress and aeroelastic effects will be important at large sweep angles (the order of 60°). Moderate thickness ratios (T = 0.08) apparently can be used in conjunction with moderate aspect ratios (up to roughly 6) at small angles of sweepback (about 30°), but the usable range of aspect ratios decreases rapidly as the angle of sweep increases. With a thickness ratio more typical of current practice (T = 0.12) fairly high aspect ratios (of the order of 8) are possible with small amounts of sweepback (about 30°) but low aspect ratios appear necessary if large amounts of sweep are desired.

As mentioned previously, the charts presented in figure 4 were obtained from considerations of wing bending alone; therefore, the variations presented in figure 10 and subsequent figures do not include the effects of torsion. The extent to which torsional distortion will modify the trends shown may be judged by reference to figure 9 or to equations (27) and (28), which define the ratio of the change in angle of attack due to torsion to the change in angle of attack due to bending. The equations rather than figure 9 should be used when the values of J/I or e differ significantly from those on which figure 9 is based. Correlation of the trends presented in figure 10 and the effects indicated by figure 9 leads to the conclusion that, whenever the loss in lift or shift in wing aerodynamic center produced by wing bending becomes large, the percentage alleviation afforded by torsional distortion is usually not great. For example, if wings with sweep angles greater than 30° are considered, wings with combinations of aspect ratio, thickness ratio, and sweep which are shown by figure 10 to result in aerodynamic-center shifts of 10 percent or greater due to wing bending would in no case have more than half of the shift compensated by torsional distortion and, in most cases, the compensation would be much less than this value. It should be remembered that the stress and aeroelastic effects could also be alleviated somewhat from those presented through use of a higher taper ratio or wing structural weight.

As indicated by the variations shown in figure 10, increases in either aspect ratio or sweep angle produce much larger percentage increases in aerodynamic-center shift due to bending than in stress.

This result shows that flexibility (in terms of its effect on longitudinal stability) tends to become more significant relative to stress at high aspect ratios and sweep angles.

Results are presented in figure 11 for a family of wings similar to that presented in figure 10 but the thickness ratio of which was held constant at 0.08 and the plan-form taper ratio of which was varied. The computed stress and aeroelastic parameters are plotted in figure 11 against aspect ratio for various values of sweep angle and plan-form taper ratio. These results indicate that for constant-chord wings aeroelastic effects are appreciable for all but fairly low aspect ratios. Decreasing the taper ratio results in a significant increase in the combinations of aspect ratio and sweepback which will not exceed given values of the aeroelastic parameters.

The manner in which plan-form taper ratio affects the relative importance of stress and the two aeroelastic effects considered herein may be investigated through reference to figure 7. The function $f_1(\lambda,\tau)$ exhibits a continuous increase with increase in taper ratio. Since this function appears in the incremental lift parameter but not in the stress parameters (see fig. 4) a progressively greater loss in lift due to wing bending relative to the stress per g normal acceleration is indicated. Correspondingly, the function $f_2(\lambda,\tau)$ which appears only in the incremental moment parameter has a rapid increase up to a taper ratio of 0.4 but little change thereafter. (See fig. 7.) This variation means that the aerodynamic-center shift due to wing bending becomes increasingly larger relative to the stress per g with increase in taper ratio at small taper ratios but there is little change with further increase in taper ratios. The variation of the ratio $f_2(\lambda,\tau)/f_1(\lambda,\tau)$ indicates the relative importance of aerodynamic-center shift and loss in lift as aeroelastic effects. Thus, the magnitude of the aerodynamic-center shift relative to loss in lift increases with increase in taper ratio up to a taper ratio of about 0.25 but then decreases with further increase in taper ratio. The relative magnitude of these two aeroelastic phenomena may be important in establishing the over-all effect of aeroelasticity on the longitudinal stability of an airplane with a horizontal tail. This point is discussed subsequently.

The effect of a linear variation in thickness ratio along the span is indicated in figure 12 where the computed stress and aeroelastic parameters are plotted against angle of sweepback for values of τ equal to 0.5 and 1.0. The wings used in this example have the same section and structural weight, operated under the same flight condition, and used the same structural material as the previous examples. These wings have an aspect ratio of 4, a symmetric parabolic-arc section, and the average of the root and tip section thickness ratios was 0.08.

A linear reduction in thickness ratio to a value at the tip of one-half that at the root, as shown in figure 12, reduces the stress and aeroelastic effects by a small amount over those which occur for the wing with a constant thickness ratio. Whether advantage could be taken of such a modification would depend upon its effect on other contributing factors in the wing selection such as drag. Reference to the variations in $f_1(\lambda,\tau)$, $f_2(\lambda,\tau)$, and $f_2(\lambda,\tau)/f_1(\lambda,\tau)$ in figure 7 indicates that tapering the thickness ratio produced a somewhat smaller ratio of loss in lift to the stress per g normal acceleration than occurred for the constant-thickness-ratio case and a slightly larger ratio of aerodynamic-center shift due to bending to stress per g normal acceleration than occurred for the constant-thickness-ratio case. The shift in aerodynamic center relative to the loss in lift is larger than for the constant-thickness-ratio case.

Effect of wing structural weight.- The effect of changing the wing structural weight is shown in figure 13. The duralumin wings assumed in this example had an aspect ratio of 4, a constant thickness ratio of 0.08, a plan-form taper ratio of 0.5, a symmetric parabolic-arc section, and operated at the same flight conditions as in previous examples. The magnitudes of the stress or aeroelastic effects are approximately in inverse proportion to the structural weight for the range of structural weights presented. For higher structural weights, these variations would be less because the wings approach a solid condition, and the increased structure afforded by the increase in weight must be added nearer the elastic axis where it does not contribute appreciably to the strength and stiffness of the wing.

Effect of structural material.- The effect of the choice of steel or duralumin as a structural material is shown in figure 14. The example wing and the flight condition are the same as those considered in the preceding section and the value of $W/S^{3/2}$ selected was 0.2. As may be seen from figure 14, very little choice can be made between these materials as far as aeroelastic considerations are concerned, although duralumin is usually considered superior on the stress-weight basis. This result with respect to aeroelastic effects is due to the fact that the increased density of steel over duralumin is offset by an almost proportional increase in modulus of elasticity. Actually, a superiority of steel wings over duralumin wings is indicated on the basis of aeroelastic considerations when the duralumin wing approaches solidity because the steel wing of the same weight would still be relatively hollow and therefore more efficient structurally.

Effect of flight condition.- The effect of changes in flight condition is shown in figure 15. The duralumin wings assumed in this example had an aspect ratio of 4, a constant thickness ratio of 0.08, a plan-form taper ratio of 0.5, a symmetric parabolic-arc section, and a

structural weight corresponding to a value of $W/S^{3/2}$ of 0.2. The computed stress and aeroelastic parameters are plotted against angle of sweepback. The curves shown in figure 15 are for three flight conditions. The basic curve is for the condition used in previous examples, a Mach number of 0.90 at an altitude of 30,000 feet. A second curve shows the effect of a reduction in altitude to sea level while maintaining the same airspeed, and a third curve shows the effect of a speed change at an altitude of 30,000 feet corresponding to a reduction in Mach number from 0.90 to 0.75. The upper plot on figure 15 indicates that there are no effects on the stress per g normal acceleration because in the method of analysis no account was taken of the effect on the stress of the inboard shift of the center of pressure due to aeroelasticity. In most cases, this effect would be small. The large increase in aeroelastic effects due to a decrease in altitude results from the change in dynamic pressure associated with the increased density. The decrease in Mach number had a slight effect for the sea-level condition. This effect is manifested by a reduction in lift-curve slope and is relieving in nature, as indicated by the equation for C_{L_α} presented previously. The figure also indicates a relatively large decrease in aeroelastic effects for a small decrease in airspeed. Again this reduction primarily reflects a decrease in dynamic pressure. A secondary effect results from reduction in lift-curve slope through reduction in Mach number.

Effect of inertia loading.- No detailed discussion can be presented as to the effects of the inertia of the wing on aeroelastic phenomena. These effects cannot be generalized in that they depend on the distribution of wing weight which can have extremely wide variations due, for example, to the presence of concentrated masses that do not contribute to the structural strength. The inertia of the wing, however, does produce a relieving effect in maneuvers which may be illustrated by assuming that the total wing weight is uniformly distributed along the span (the same assumption as for the aerodynamic loading). Under these conditions the inertia loading p_i is given by

$$p_i = -\frac{W_w n}{S}$$

and the aerodynamic loading p_a is given by

$$p_a = \frac{W_G n}{S}$$

The total loading then is

$$p = \frac{W_G n}{S}\left(1 - \frac{W_W}{W_G}\right)$$

$$= C_L q\left(1 - \frac{W_W}{W_G}\right)$$

For most airplanes having a fuselage and relatively thin wings W_W/W_G is small compared to unity. This condition gave rise to the assumption used herein that only the aerodynamic loading (first term in the foregoing equation) be considered in the present analysis. The foregoing equation shows, as is well-known, that the wing weight tends to reduce the loading which produces the aeroelastic distortion. In cases where the weight contained within the wings is large compared with the gross weight (the flying wing, for example), this relieving effect would be extremely beneficial. Advantage may be taken of corresponding effects of concentrated loads through judicious location of engine nacelles and external stores.

Effects involving the complete airplane.- The previous discussion has been concerned with the effects of aeroelasticity on the wing itself. When the over-all effects to be expected on an airplane with a horizontal tail are considered, further discussion is appropriate. The results obtained herein for a wing can be applied to a horizontal tail as well, but other effects on the complete airplane, such as bending of the fuselage or the induction effects caused by the downwash changes at the tail produced by wing distortion, cannot be analyzed by the present method. These latter effects are usually smaller than the effects caused by distortion of the wing and tail, however, and the discussion is thus confined to these two components. Effects of both horizontal-tail and fuselage flexibility on longitudinal control are considered in reference 7 and similar effects on longitudinal stability are also considered briefly.

The wing-aerodynamic-center shift caused by aeroelastic effects directly reflects a change in the longitudinal stability of a flying-wing airplane. The change in the longitudinal stability of an airplane with a horizontal tail is in turn related to a shift in the point for neutral stability with respect to angle of attack. This neutral point is not only affected by the wing-aerodynamic-center shift but also by other factors. This condition may be seen from the following equation which expresses this shift

$$\frac{\Delta x_n}{\overline{c}} = \frac{\Delta \overline{x}}{\overline{c}} + \frac{\left(C_{L_{\alpha_t}}\right)_R}{\left(C_{L_{\alpha_w}}\right)_R} \left[1 - \frac{\dfrac{\left(C_{L_{\alpha_t}}\right)_F}{\left(C_{L_{\alpha_t}}\right)_R}}{\dfrac{\left(C_{L_{\alpha_w}}\right)_F}{\left(C_{L_{\alpha_w}}\right)_R}}\right] \left(1 - \frac{d\epsilon}{d\alpha}\right)\frac{q_t}{q}\frac{S_t}{S}\frac{l}{\overline{c}}$$

The pertinent assumptions made in deriving the foregoing expression are that the aerodynamic-center shift due to wing bending $\Delta \overline{x}/\overline{c}$ is the same for the wing-body combination as for the wing alone, that the distance between the point for neutral stability and the tail center of pressure l is the same for the rigid airplane and the flexible airplane, and that the variation of downwash angle at the tail with angle of attack $d\epsilon/d\alpha$ is not affected by the wing distortion. This equation shows that the neutral-point shift is dependent on a term involving the effect of flexibility on the lift-curve slopes of the wing and horizontal tail as well as a term involving the shift in aerodynamic center of the wing.

For the case where $\left(C_{L_{\alpha_t}}\right)_F\!\!\Big/\!\left(C_{L_{\alpha_t}}\right)_R$ is equal to $\left(C_{L_{\alpha_w}}\right)_F\!\!\Big/\!\left(C_{L_{\alpha_w}}\right)_R$ (a condition which might conceivably be called equal flexibility of wing and tail), the foregoing equation shows that the shift in neutral point is the same as the shift in the aerodynamic center of the wing. For the case where $\left(C_{L_{\alpha_t}}\right)_F\!\!\Big/\!\left(C_{L_{\alpha_t}}\right)_R$ is greater than $\left(C_{L_{\alpha_w}}\right)_F\!\!\Big/\!\left(C_{L_{\alpha_w}}\right)_R$ (the tail effectively stiffer than the wing), the second term in the foregoing equation becomes negative and tends to compensate for the positive shift in wing aerodynamic center produced by aeroelastic distortion. Presumably, if such a condition exists, it should be possible to adjust such factors as S_t/S or $l/\overline{c}$ until the wing-aerodynamic-center shift is completely compensated. The physical interpretation of the condition is that the wing would be so positioned on the fuselage that the center of pressure of the loss in lift for the complete airplane caused by aeroelastic action would be at the point of neutral static stability for the rigid airplane, and therefore no shift in this point would occur because of flexibility. Generally, it would be more feasible to keep the tail length l constant and to adjust the tail size to accomplish this end.

If the horizontal tail is assumed to be rigid the tail size required for complete compensation of the aeroelastic effects considered can be obtained by equating the expression for the location of the center of pressure of the loss in wing lift previously derived (eq. (16)) to the expression for the center-of-gravity position for neutral static stability of the rigid airplane. With a flexible tail, a different

relation would apply, and the effect of tail flexibility is discussed in more detail subsequently. Equating the expressions as stated previously gives

$$\frac{x_n}{\bar{c}} = \frac{(x_{cp})_{\Delta L}}{\bar{c}}$$

$$\left(\frac{\bar{x}}{\bar{c}}\right)_{wb} - \frac{\left(C_{L\alpha_t}\right)_R}{\left(C_{L\alpha}\right)_R}\left(1 - \frac{d\epsilon}{d\alpha}\right)\frac{q_t}{q}\frac{S_t}{S}\frac{l}{\bar{c}} = -0.25 + A\frac{f_2(\lambda,\tau)}{f_1(\lambda,\tau)}\tan\Lambda$$

In order to express the various lengths appearing in this equation in terms of a general length dimension rather than the chord, the following expression is substituted:

$$\bar{c} = \sqrt{\frac{S}{A}}\ f_3(\lambda)$$

Solving for the area ratio gives

$$\frac{S_t}{S} = \frac{0.25\dfrac{\bar{c}}{\sqrt{S}} + \dfrac{\bar{x}}{\sqrt{S}} - \sqrt{A}\ f_3(\lambda)\dfrac{f_2(\lambda,\tau)}{f_1(\lambda,\tau)}\tan\Lambda}{\dfrac{\left(C_{L\alpha_t}\right)_R}{\left(C_{L\alpha}\right)_R}\left(1 - \dfrac{d\epsilon}{d\alpha}\right)\dfrac{q_t}{q}\dfrac{l}{\sqrt{S}}}$$

When more or less typical values for the parameters in this equation are assumed, area ratios have been calculated for various aspect ratios and angles of sweepback. These area ratios are presented in figure 16. The assumed values of the parameters are as follows:

$$0.25\frac{\bar{c}}{\sqrt{S}} + \frac{\bar{x}}{\sqrt{S}} = 0.06 \qquad\qquad \frac{l}{\sqrt{S}} = 1.2$$

$$\lambda = 0.5 \qquad\qquad \frac{d\epsilon}{d\alpha} = 0.4$$

$$\frac{\left(C_{L\alpha_t}\right)_R}{\left(C_{L\alpha}\right)_R} = 0.85 \qquad\qquad \frac{q_t}{q} = 1.0$$

The value of $0.25 \dfrac{\bar{c}}{\sqrt{S}} + \dfrac{\bar{x}}{\sqrt{S}}$ is typical for a wing-fuselage combination rather than for a wing alone. The center of pressure of the loss in wing lift is also presented in figure 16 as a function of aspect ratio and sweepback angle.

The results presented in figure 16 show that the tail size required for complete compensation of the wing aeroelastic effects on longitudinal stability increases somewhat with increase in aspect ratio. The tail size increases much more rapidly with increase in sweepback angle, particularly at large sweepback angles. In general, the tail sizes required for this complete compensation would appear prohibitive except at small angles of sweepback. Usual tail-wing area ratios are of the order of 0.2 and the aerodynamic efficiency of an airplane is known to decrease as the size of the horizontal tail increases. Reference again to figure 16 indicates that for most conditions the center of pressure of the loss in wing lift is further back than the neutral-point locations for most airplanes. Location of the point for neutral stability with respect to angle of attack usually ranges from $30\bar{c}$ to $50\bar{c}$ back of the leading edge of the mean aerodynamic chord. It does not appear, however, that rearrangement of the airplane configuration to provide satisfactory static margins with extremely rearward center-of-gravity positions would be particularly difficult from the standpoint of rearranging the weight distribution; the large tail-size requirement would be the most serious limitation. The possibility for obtaining complete compensation appears even more remote when a flexible tail is considered. For any given wing sweepback angle and aspect ratio the tail size required for complete compensation increases rapidly with increased tail flexibility until, when the wing and tail are equally flexible, no compensation for the wing-aerodynamic-center shift is possible regardless of tail size. As would be expected if the horizontal tail is more flexible than the wing, the presence of the tail is detrimental from the aeroelastic standpoint and increase in tail size would result in increased effects of aeroelasticity on the longitudinal stability of the airplane. On the other hand, whenever the horizontal tail is effectively stiffer than the wing, some degree of compensation is always obtained.

CONCLUSIONS

An analysis has been made of factors affecting the loss in lift and the shift in aerodynamic center of a wing produced by the wing bending under aerodynamic load. The analysis was applied to shell-wing structures in which the spanwise variation in skin thickness is of a character to give a constant spanwise stress under a uniformly distributed load. Conclusions obtained from the results of this analysis are as follows:

1. The geometric parameters the variations of which produce the largest changes in the aeroelastic effects considered herein are aspect ratio, sweepback angle, and section thickness ratio. Based on the weight of current wing structures, consideration of the effects of wing bending alone leads to the conclusion that for sweptback wings with low values of section thickness ratio (0.04) the aeroelastic effects are extreme for all but low aspect ratios (2) and even then the effects are large for large angles of sweepback (60°). The effects of wing flexibility on the longitudinal stability of an airplane become more important relative to considerations of wing stress as the aspect ratio or sweepback angle of the wing is increased or the thickness ratio decreased.

2. The effects of torsional flexibility on loss in wing lift and shift in aerodynamic center will usually tend to alleviate the effect of bending, but the alleviation afforded will not be large in general because the angle-of-attack changes due to torsion will usually be much smaller than those due to bending except for wings with low values of sweep, aspect ratio, or, in particular, a combination of the two.

3. Reducing the plan-form taper ratio reduces the aeroelastic effects considerably. The reduction in the shift in aerodynamic center resulting from decrease in taper ratio is about the same as the reduction in stress for all but very low taper ratios where the reduction in the shift of the aerodynamic center is much greater than the reduction in stress. The reduction in loss in lift through reduction in taper ratio is larger than the reduction in stress for all ranges of plan-form taper ratio.

4. For wings having a constant extreme-fiber stress along the span, the alterations in aeroelastic effects produced by variations in section thickness ratio along the span and by practical variations in airfoil shape are small.

5. Of the factors dependent on flight condition, dynamic pressure is the most important from the standpoint of aeroelastic effects. For the cases considered, Mach number effects exist chiefly in the manner in which the lift-producing effectiveness of the wing is altered.

6. An increase in wing weight per unit area with increase in size appears to be more difficult to prevent when aeroelastic effects are an important consideration than when stress alone is a consideration. For the type of structure considered herein and for any given wing material and external geometry, the loss in lift and aerodynamic-center shift are approximately in inverse proportion to the structural weight except when the wing is nearly solid. Under the latter condition, the effects of changes in wing structural weight are reduced.

7. On the basis of the aeroelastic effects considered, there appears to be little choice between steel and duralumin as a structural material except for conditions when the duralumin wing approaches solidity;

the steel wing of the same weight would still be relatively hollow and therefore superior because of its higher structural efficiency.

8. In maneuvers the aeroelastic effects produced by the aerodynamic loading are alleviated somewhat by the inertia of the wing.

9. The effects of loss in wing lift and shift in its aerodynamic center on the static longitudinal stability of an airplane with a horizontal tail are dependent on the flexibility of the horizontal tail. If it is assumed that the fuselage flexibility is small and that the effect of wing flexibility on the variation with angle of attack of the downwash at the tail can be neglected, the following conclusions apply:

(a) The shift in wing aerodynamic center is approximately equal to the shift in the center-of-gravity position for neutral stability with respect to angle of attack when the loss in lift of the wing and tail are equal.

(b) The shift in wing aerodynamic center is usually somewhat greater than the shift in center-of-gravity position for neutral stability with respect to angle of attack when the loss in lift of the tail is less than that of the wing.

Langley Aeronautical Laboratory,
    National Advisory Committee for Aeronautics,
        Langley Field, August 15, 1952.

APPENDIX

THE EFFECT OF SPANWISE DISTRIBUTION OF LOADING ON THE

SPANWISE VARIATION OF ANGLE-OF-ATTACK

CHANGE DUE TO BENDING

In order to illustrate the effect of various distributions of span-
wise loading on the angle of attack due to bending, two extreme loading
conditions were investigated and the angle-of-attack variations were
obtained and compared with those obtained for a constant loading condi-
tion assumed in the present report. The conditions investigated are
(1) the load varies linearly from root to tip, the tip-chord loading
being 50 percent less than the root-chord loading, and (2) the load
varies linearly, the tip-chord loading being 50 percent greater than the
root-chord loading. Parameters applying to the first extreme-loading
condition are denoted by the subscript 1; parameters applying to the
second extreme-loading condition are denoted by the subscript 2; and
the parameters applying to the constant loading condition have no sub-
script. For these calculations a constant thickness ratio was assumed.
In order to analyze the problem, the following relations were used to
determine the ratios of the angle-of-attack changes along the span
(see expression following eq. 6):

$$\Delta\alpha_B = - \frac{dz'}{dy'} \sin \gamma$$

where

$$\frac{dz'}{dy'} = \frac{2s'}{ET'} \int_0^{y'/s'} \frac{\sigma_{y'}}{c'} d\frac{y'}{s'}$$

The ratios of angle-of-attack changes are then found as

$$\frac{(\Delta\alpha_B)_1}{\Delta\alpha_B} = \frac{\left(\frac{dz'}{dy'}\right)_1}{\frac{dz'}{dy'}} = \frac{\int_0^{y'/s'} \frac{(\sigma_{y'})_1}{c'} d\frac{y'}{s'}}{\int_0^{y'/s'} \frac{\sigma_{y'}}{c'} d\frac{y'}{s'}} \tag{A1}$$

The stress ratios are proportional to the ratios of the bending moment and are

$$\left(\sigma_{y'}\right)_1 = \frac{\left(\sigma_{y'}\right)_1}{\sigma_{y'}}\,\sigma_{y'} = \frac{M_{B_1}}{M_B}\,\sigma_{y'}$$

Since the wings were designed for a constant spanwise stress for the constant-loading condition, equation (A1) may be expressed

$$\frac{\left(\Delta\alpha_B\right)_1}{\Delta\alpha_B} = \frac{\displaystyle\int_0^{y'/s'} \frac{M_{B_1}}{c'M_B}\,d\frac{y'}{s'}}{\displaystyle\int_0^{y'/s'} \frac{d\frac{y'}{s'}}{c'}} = \frac{\displaystyle\int_0^{y'/s'} \frac{1}{\left[1 - (1 - \lambda)\frac{y'}{s'}\right]}\frac{M_{B_1}}{M_B}\,d\frac{y'}{s'}}{\displaystyle\int_0^{y'/s'} \frac{1}{\left[1 - (1 - \lambda)\frac{y'}{s'}\right]}\,d\frac{y'}{s'}} \qquad (A2)$$

The moment at any spanwise station is obtained from the following equation (see eq. 1):

$$M_B = \int_y^{s'} pc'_\xi \xi(\xi - y')\,d\xi \qquad (A3)$$

where

$$c'_\xi = c'_r\left[1 - (1 - \lambda)\frac{\xi}{s'}\right]$$

When the indicated integration is performed, the moment relation for the constant-loading case becomes

$$M_B = pc'_r(s')^2\left[\frac{1 + 2\lambda}{6} - \frac{1 + \lambda}{2}\frac{y}{s} + \frac{1}{2}\left(\frac{y}{s}\right)^2 - \frac{1 - \lambda}{6}\left(\frac{y}{s}\right)^3\right] \qquad (A4)$$

For the first extreme-loading condition the loading varies linearly from the root chord to tip chord with the tip section loading 50 percent less than the root section loading. The total load is the same as for the constant-loading case. The relation of the loadings is expressed as

$$\int_0^{s'} p_1 c' \, dy' = L = \int_0^{s'} pc' \, dy' \tag{A5}$$

where under the assumed loading condition

$$p_1 = K_1 \left(1 - \frac{1}{2} \frac{y}{s} \right) \tag{A6}$$

Substituting equation (A6) into equation (A5) and then integrating gives the following relation

$$K_1 \left(s' - \frac{1 - \lambda}{2} s' - \frac{1}{4} s' + \frac{1 - \lambda}{6} s' \right) = p \left(s' - \frac{1 - \lambda}{2} s' \right)$$

Solution of this equation for the loading constant K_1 yields

$$K_1 = \frac{6 + 6\lambda}{5 + 4\lambda} p \tag{A7}$$

When the relation (A6) is substituted into equation (A3) and then integrated, the moment M_{B_1} is obtained for the first extreme-loading condition

$$M_{B_1} = \frac{1}{2} \frac{1 + \lambda}{5 + 4\lambda} pc'_r (s')^2 \left[\frac{3 + 5\lambda}{2} - (5 + 4\lambda)\frac{y}{s} + 6\left(\frac{y}{s}\right)^2 - \right.$$

$$\left. (3 - 2\lambda)\left(\frac{y}{s}\right)^3 + \frac{1 - \lambda}{2}\left(\frac{y}{s}\right)^4 \right] \tag{A8}$$

The expressions for M_{B_1} and M_B were substituted into equation (A2) and the indicated integration performed graphically for taper ratios of zero and unity. Curves showing the values of $\dfrac{(\Delta\alpha_B)_1}{\Delta\alpha_B}$ along the span for these two taper ratios are presented in figure 17.

For the second extreme-loading condition the loading varies linearly and the tip-section loading is 50 percent greater than the root-section loading. The relation of the loading is expressed in equation form as

$$\int_0^{s'} p_2 c'\, dy' = W = \int_0^{s'} pc'\, dy' \tag{A9}$$

where under the assumed loading condition

$$p_2 = K_2\left(1 + \frac{1}{2}\frac{y}{s}\right) \tag{A10}$$

As for the previous condition the loading constant was determined and is as follows:

$$K_2 = \frac{6 + 6\lambda}{7 + 8\lambda}\, p \tag{A11}$$

When the relation (A10) is substituted into equation (A3) and then integrated, the bending moment M_{B_2} is obtained for the second extreme condition of loading

$$M_{B_2} = \frac{1}{2}\frac{1 + \lambda}{7 + 8\lambda} pc'_r(s')^2\left[\frac{5 + 11\lambda}{2} - (7 + 8\lambda)\frac{y}{s} + 6\left(\frac{y}{s}\right)^2 - \right.$$

$$\left. (1 - 2\lambda)\left(\frac{y}{s}\right)^3 - \frac{1 - \lambda}{2}\left(\frac{y}{s}\right)^4\right] \tag{A12}$$

The expressions for M_{B_2} and M_B were substituted into equation (A2) $\left(M_{B_2} \text{ in place of } M_{B_1} \right)$ and the indicated integrations performed graphically for taper ratios of zero and unity. Curves showing the values of $\dfrac{\left(\Delta \alpha_B \right)_2}{\Delta \alpha_B}$ along the span are also presented in figure 17.

The variations of $\dfrac{\left(\Delta \alpha_B \right)_1}{\Delta \alpha_B}$ and $\dfrac{\left(\Delta \alpha_B \right)_2}{\Delta \alpha_B}$ are not presented outboard of the 0.8-semispan station. Near the tip the variations obtained by the method used in this appendix are not significant because the assumed loading and the variation of skin thickness in this region are not representative of the practical case. The conditions near the tip were modified for the constant-loading case used in the present report in order to account for these effects (see discussion of angle-of-attack change due to bending in the section entitled "Method of Analysis"). If similar modifications were made for the cases of extreme loading considered here, the variations shown in figure 17 would approach a constant value (zero slope) at the tip for finite taper ratios. The calculated variations are considered realistic inboard of the 0.8-semispan station. In this range the variations presented show that the effect of load distribution is greater for the case of zero taper ratio than for the case of unit taper ratio and, as would be expected, is greater near the tip than near the root. The magnitude of the effects of these alterations in load distribution from that assumed in the present paper (20- to 25-percent change in $\Delta \alpha_B$ for outboard stations) are large enough to affect the preciseness of the quantitative results obtained by the method of analysis used in the present report but would not appear to affect the qualitative results.

REFERENCES

1. Diederich, Franklin W.: Calculation of the Aerodynamic Loading of
     Swept and Unswept Flexible Wings of Arbitrary Stiffness. NACA
     Rep. 1000, 1950. (Supersedes NACA TN 1876.)

2. Skoog, Richard B., and Brown, Harvey H.: A Method for the
     Determination of the Spanwise Load Distribution of a Flexible Swept
     Wing at Subsonic Speeds. NACA TN 2222, 1951.

3. Miles, John W.: A Formulation of the Aeroelastic Problem for a Swept
     Wing. Jour. Aero. Sci., vol. 16, no. 8, Aug. 1949, pp. 477-490.

4. Diederich, Franklin W., and Foss, Kenneth A.: Charts and Approximate
     Formulas for the Estimation of Aeroelastic Effects on the Loading
     of Swept and Unswept Wings. NACA TN 2608, 1952.

5. Toll, Thomas A., and Queijo, M. J.: Approximate Relations and Charts
     for Low-Speed Stability Derivatives of Swept Wings. NACA TN 1581,
     1948.

6. DeYoung, John, and Harper, Charles W.: Theoretical Symmetric Span
     Loading at Subsonic Speeds for Wings Having Arbitrary Plan Form.
     NACA Rep. 921, 1948.

7. Collar, A. R., and Grinsted, F.: The Effects of Structural
     Flexibility of Tailplane, Elevator, and Fuselage on Longitudinal
     Control and Stability. R. & M. No. 2010, British A.R.C., 1942.
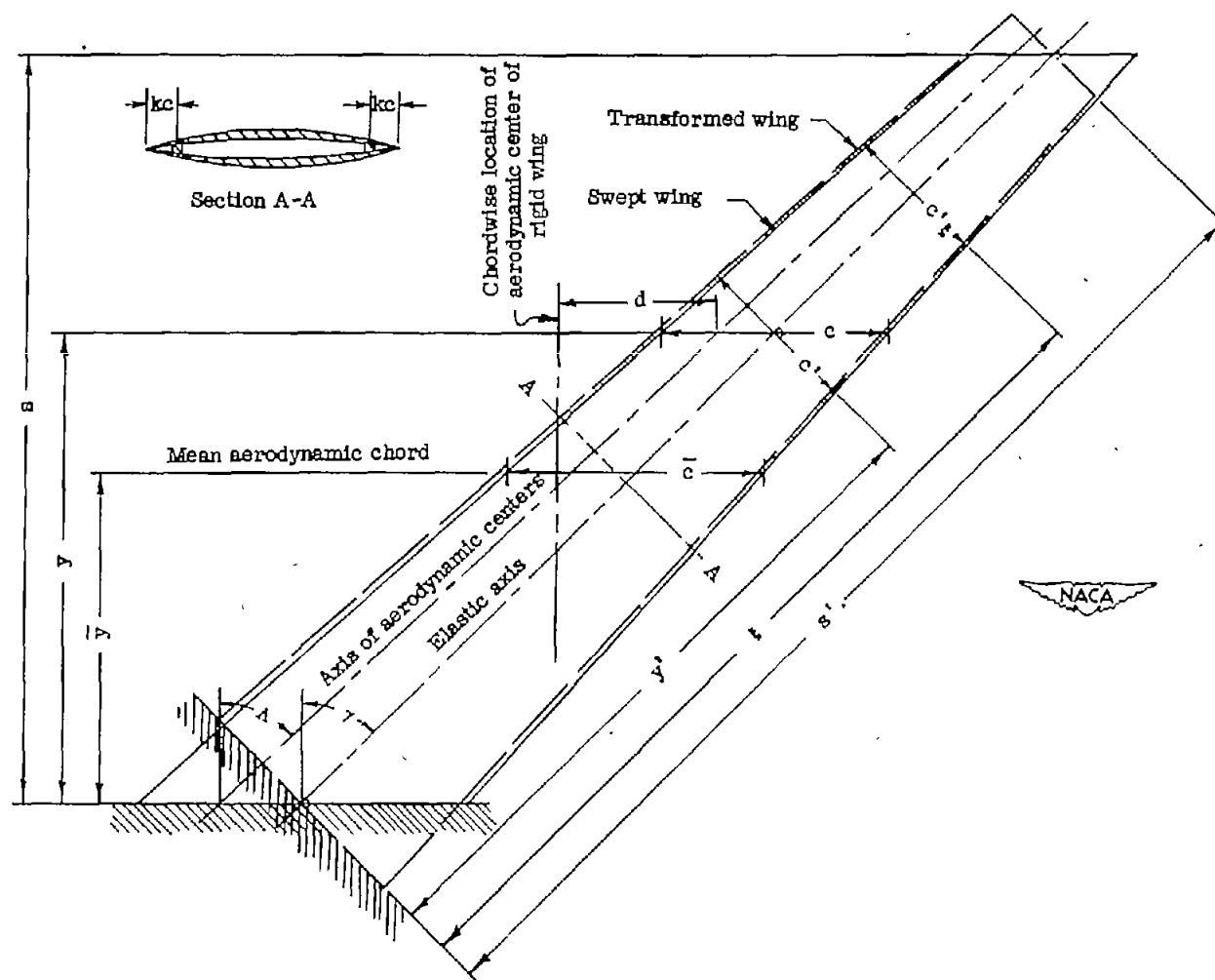
Figure 1.- Typical swept wing showing dimensions and the transformation used in the present analysis. $y' = \dfrac{y}{\cos \gamma}$; $c' = c \cos \gamma$; $s' = \dfrac{s}{\cos \gamma}$.
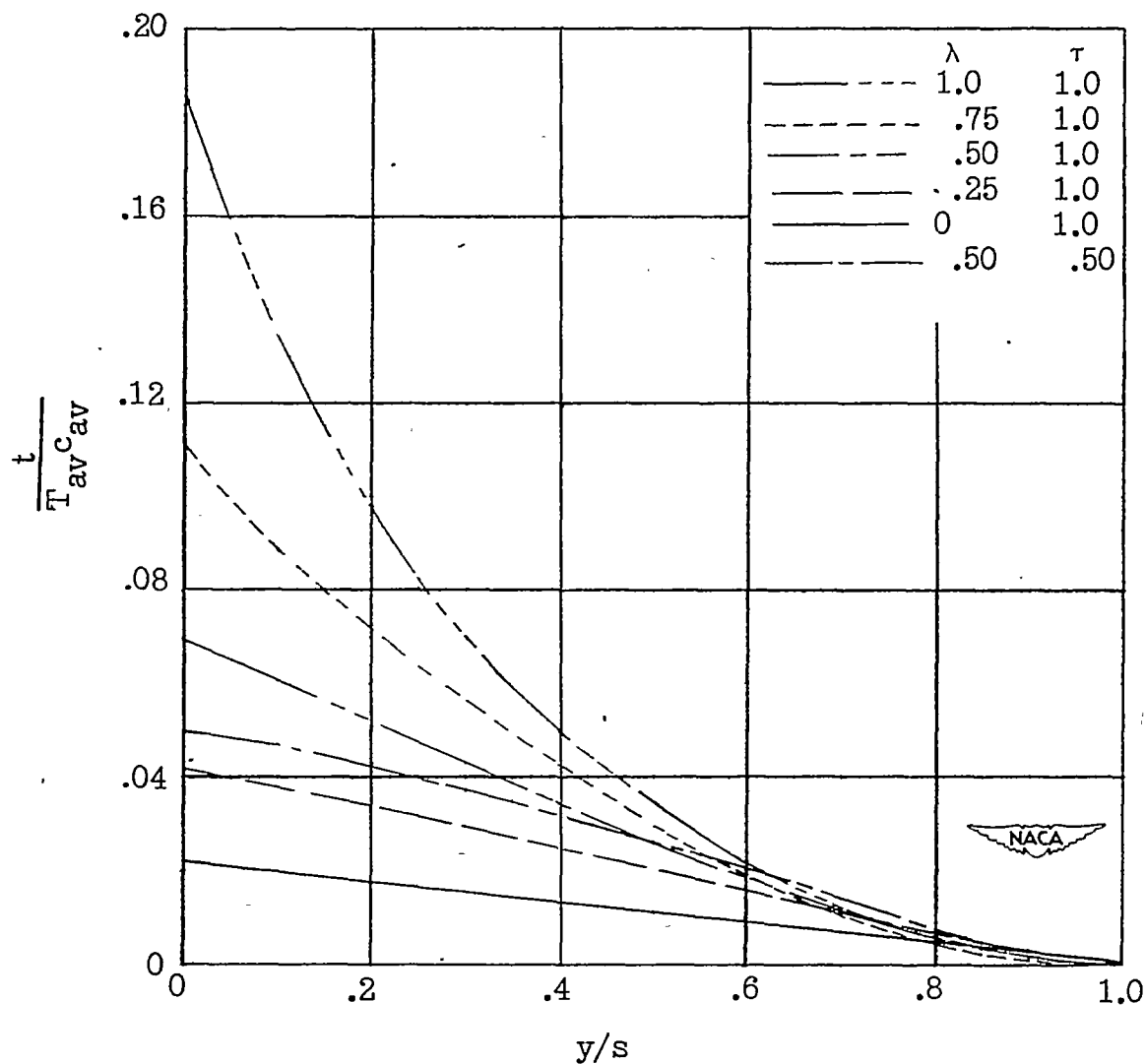
Figure 2.- Typical spanwise variations for the assumed wing structure of the ratio of skin thickness to local airfoil section thickness for various plan-form and thickness taper ratios. $\dfrac{W_G/S}{\dot{\sigma}/n}\ \dfrac{1}{I_o}\left(\dfrac{A}{T_{av}\cos\gamma}\right)^2 = 12$.
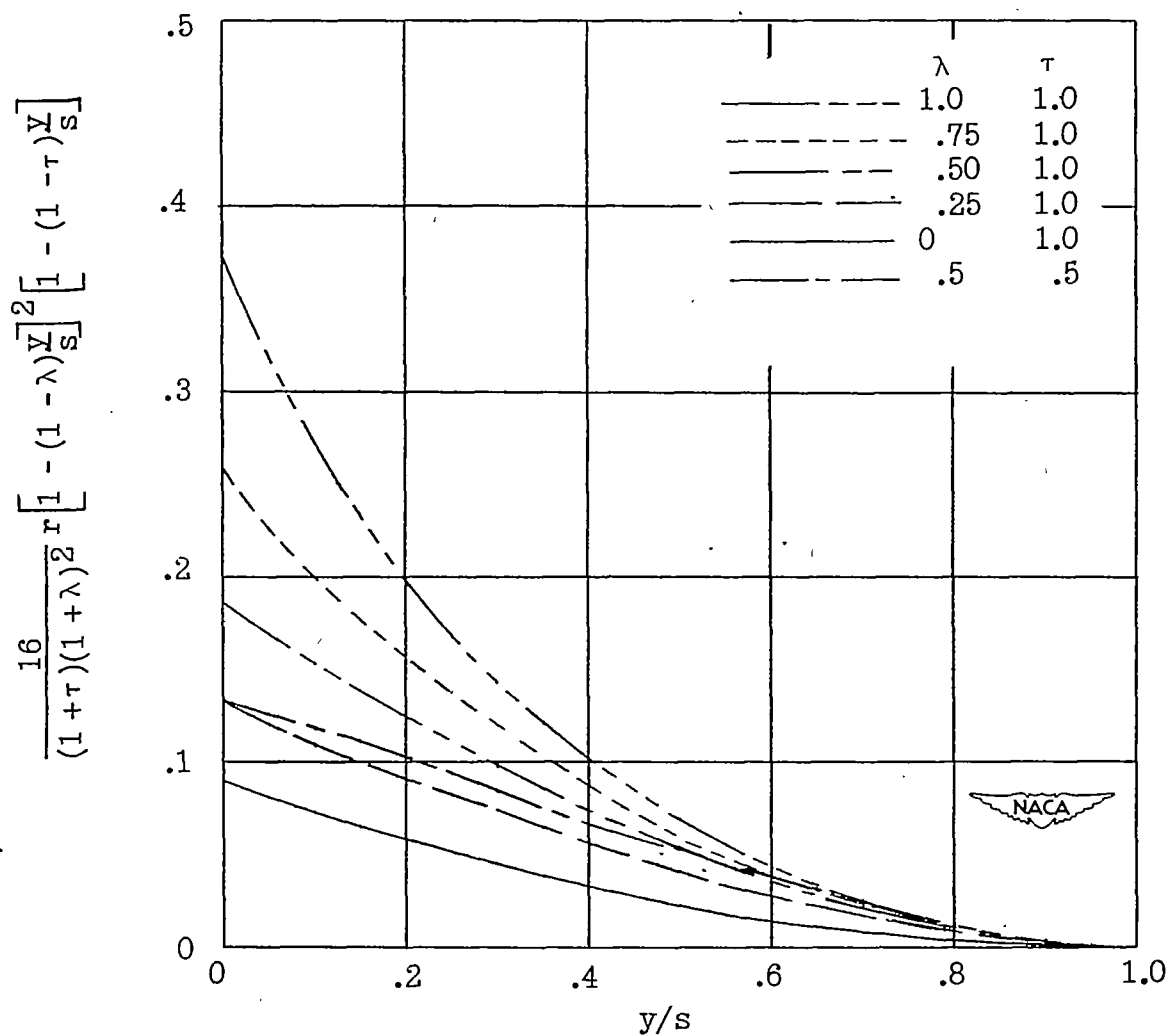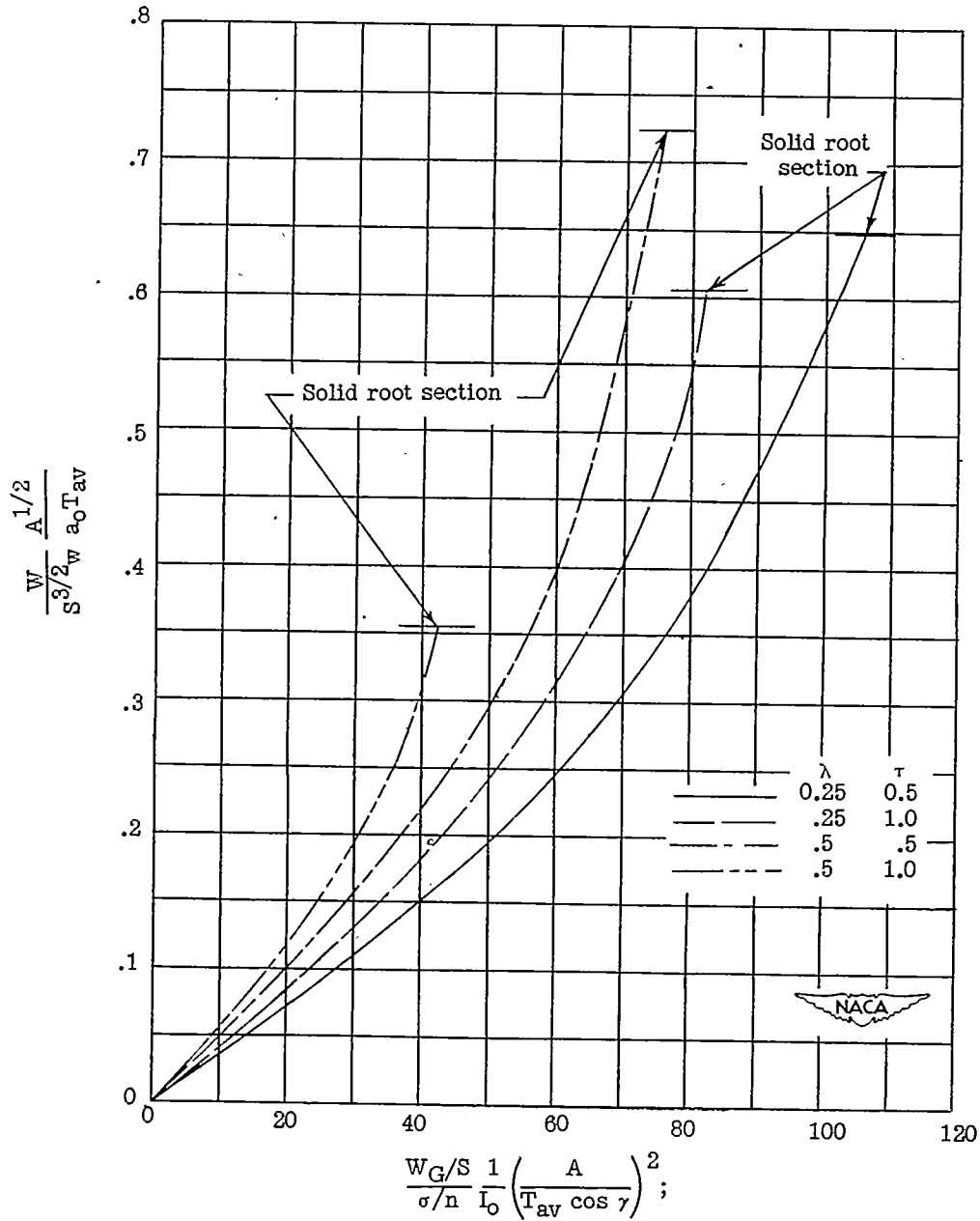
Figure 3.- Typical spanwise variations for the assumed wing structure of incremental wing weight parameter for various plan-form and thickness taper ratios. $\dfrac{W_G/S}{\sigma/n}\ \dfrac{1}{I_o}\left(\dfrac{A}{T_{av}\ \cos\ \gamma}\right)^2 = 12.$

$$\frac{W_G/S}{q/n} \frac{1}{I_o} \left(\frac{A}{T_{av} \cos \gamma}\right)^2 ;$$

$$\frac{1}{\Delta C_L/C_L} \frac{q}{EI_o} \left(\frac{A}{T_{av}}\right)^3 \left(C_{L\alpha}\right)_R \frac{\tan \gamma}{\cos^2 \gamma} f_1(\lambda, \tau); \text{ or}$$

$$\frac{1}{\Delta C_m/C_L} \frac{q}{EI_o} \frac{A^4}{T_{av}^3} \left(C_{L\alpha}\right)_R \frac{\tan \gamma \tan \Lambda}{\cos^2 \gamma} f_2(\lambda, \tau)$$

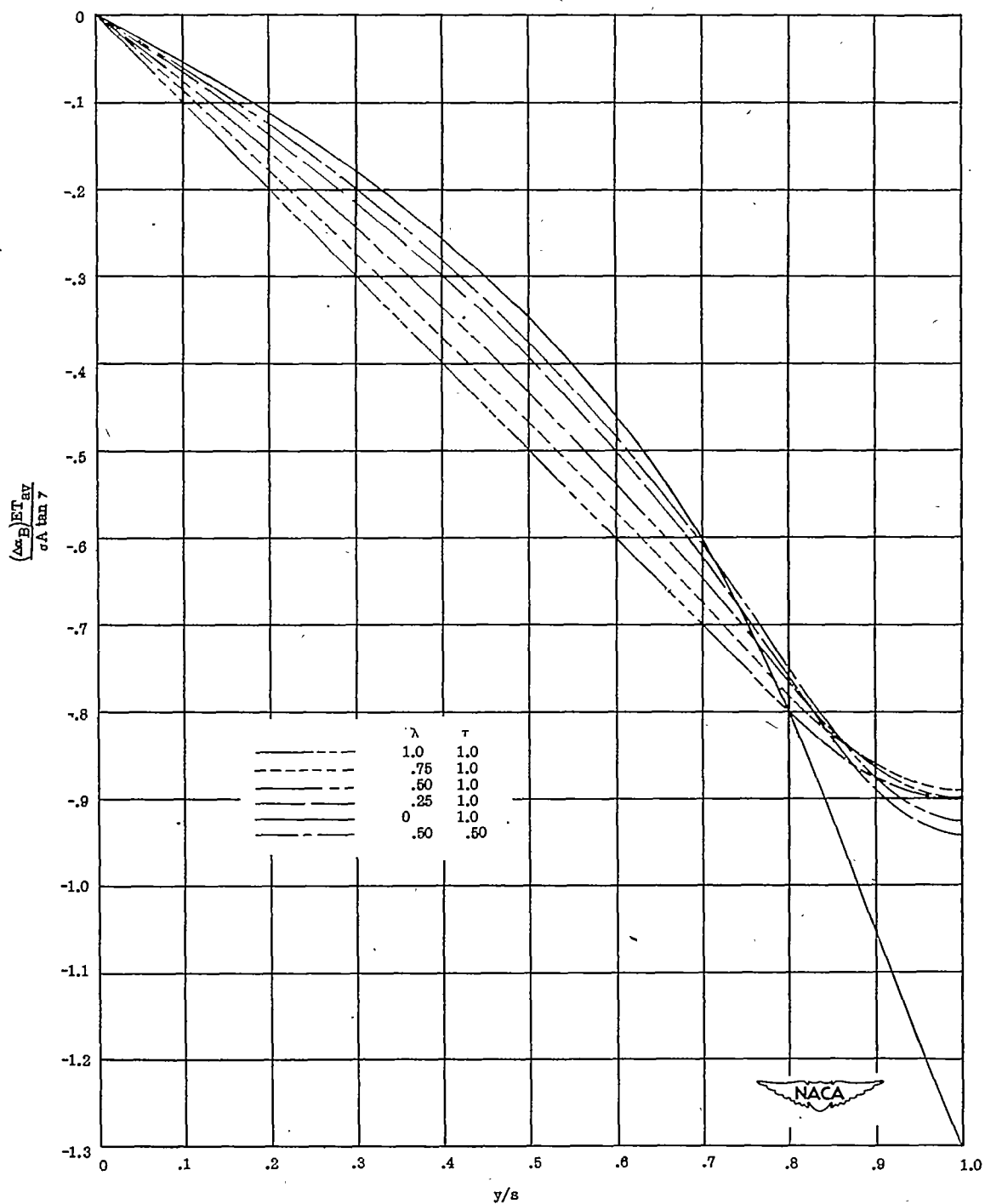(a) Plan-form taper ratio 0; thickness taper ratios 1.0 and 0.5.

Figure 4.- Variation of wing weight parameter with stress, additional
lift, or incremental moment parameter.

$$\frac{W}{S^{3/2}_W}\frac{A^{1/2}}{a_o T_{av}}$$

Vertical axis label for the chart; horizontal axis and curve legend:

λ	τ
0.25	0.5
.25	1.0
.5	.5
.5	1.0

$$\frac{W_{G}/S}{\sigma/n}\frac{1}{I_o}\left(\frac{A}{T_{av}\cos\gamma}\right)^2;$$

$$\frac{1}{\Delta C_L/C_L}\frac{q}{EI_o}\left(\frac{A}{T_{av}}\right)^3 (C_{L_\alpha})_R \frac{\tan\gamma}{\cos^2\gamma} f_1(\lambda,\tau); \text{ or}$$

$$\frac{1}{\Delta C_m/C_L}\frac{q}{EI_o}\frac{A^4}{T_{av}^3}(C_{L_\alpha})_R \frac{\tan\gamma \tan\Lambda}{\cos^2\gamma} f_2(\lambda,\tau)$$

(b) Plan-form taper ratios 0.25 and 0.50; thickness taper
ratios 1.0 and 0.50.

Figure 4.- Continued.

$$\frac{W_G/S}{\sigma/n}\left(\frac{A}{I_0 T_{av}\cos\gamma}\right)^2;$$
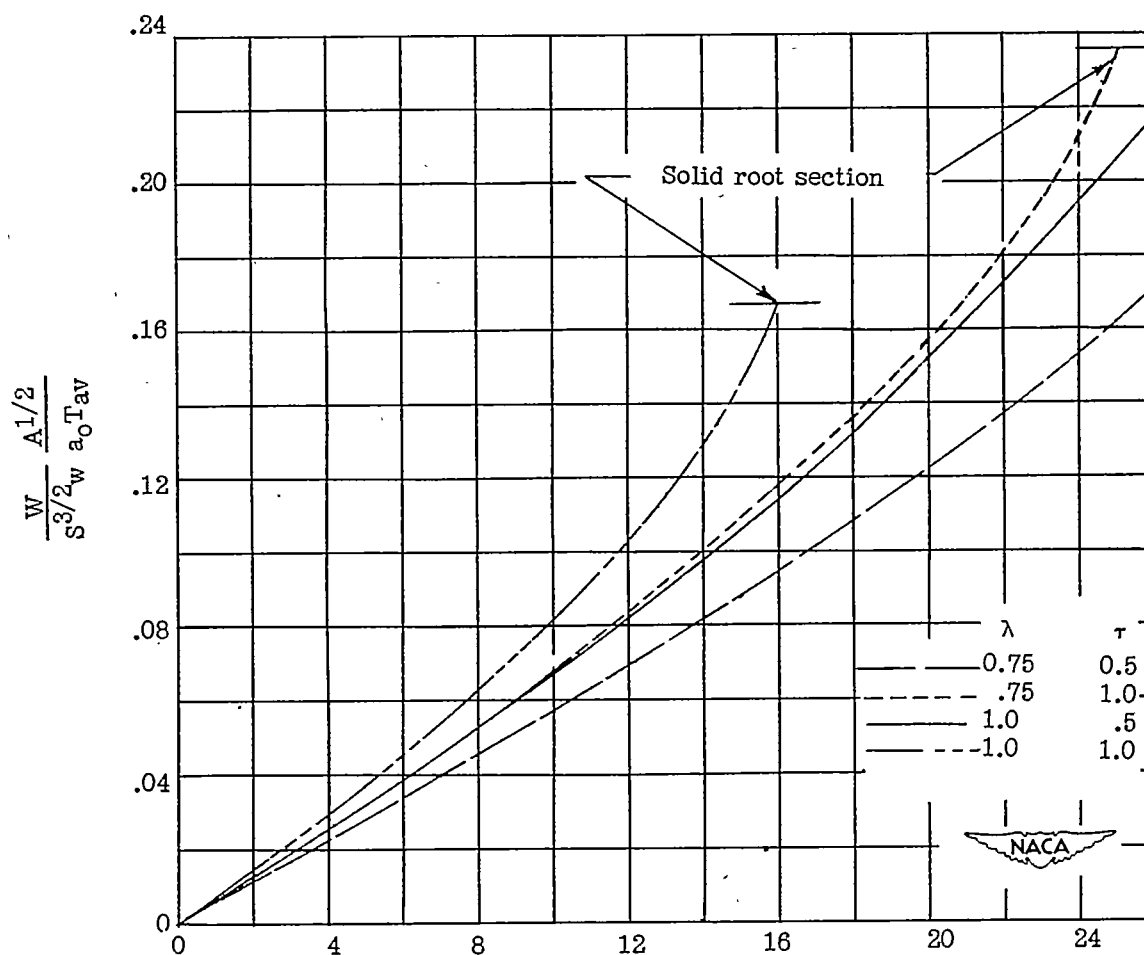
$$\frac{1}{\Delta C_L/C_L}\frac{q}{EI_0}\left(\frac{A}{T_{av}}\right)^3 \left(C_{L\alpha}\right)_R \frac{\tan\gamma}{\cos^2\gamma}f_1(\lambda,\tau); \text{ or}$$

$$\frac{1}{\Delta C_m/C_L}\frac{q}{EI_0}\frac{A^4}{T_{av}^3}\left(C_{L\alpha}\right)_R \frac{\tan\gamma\tan\Lambda}{\cos^2\gamma}f_2(\lambda,\tau)$$

(c) Plan-form taper ratios 0.75 and 1.0; thickness taper
ratios 1.0 and 0.50.

Figure 4.- Concluded.

Figure 5.- Typical spanwise variations of the change in the angle of attack produced by wing bending for various plan-form and thickness taper ratios.
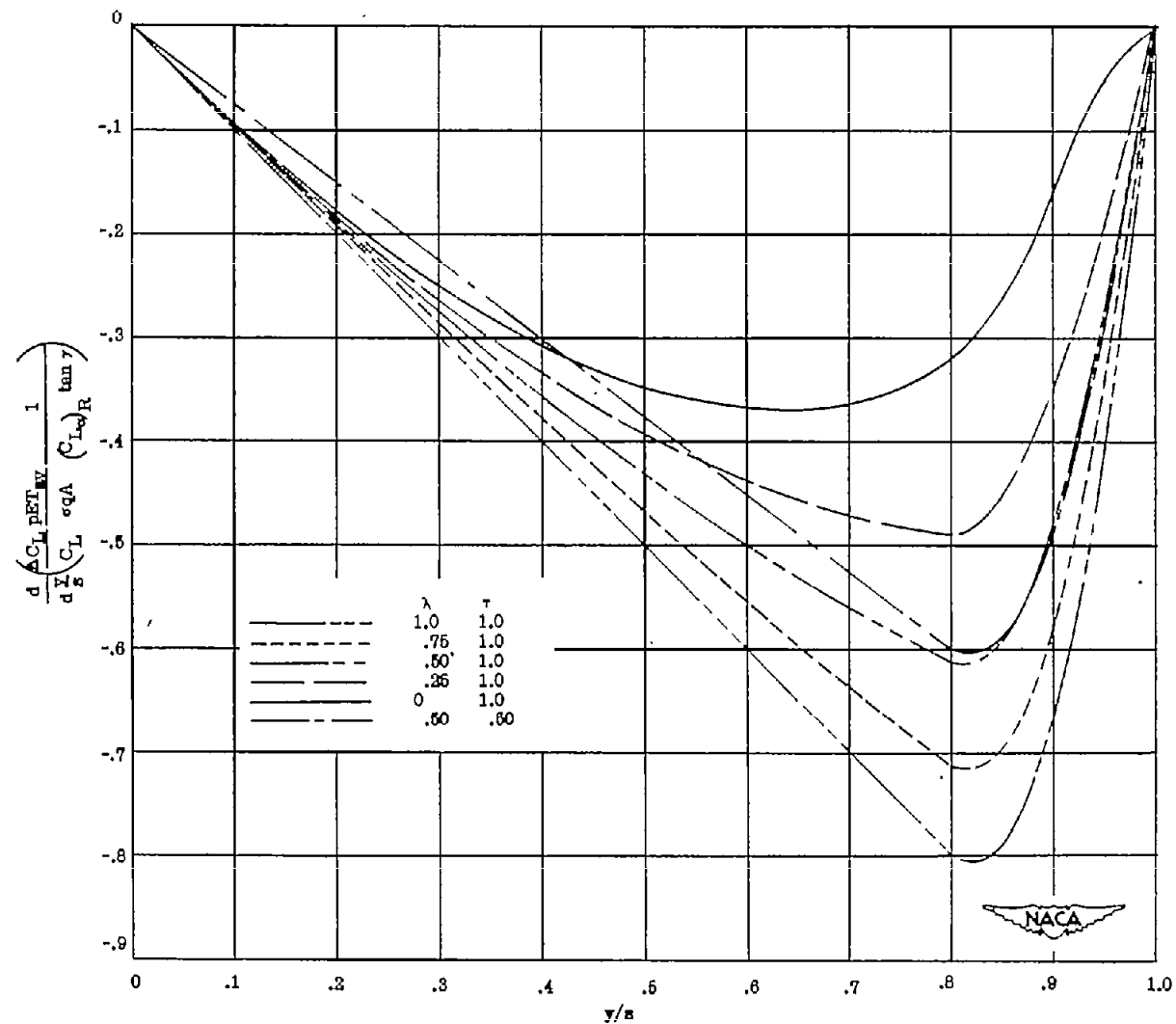
Figure 6.- Typical spanwise variations of the change in lift produced by wing bending for various plan-form and thickness taper ratios.
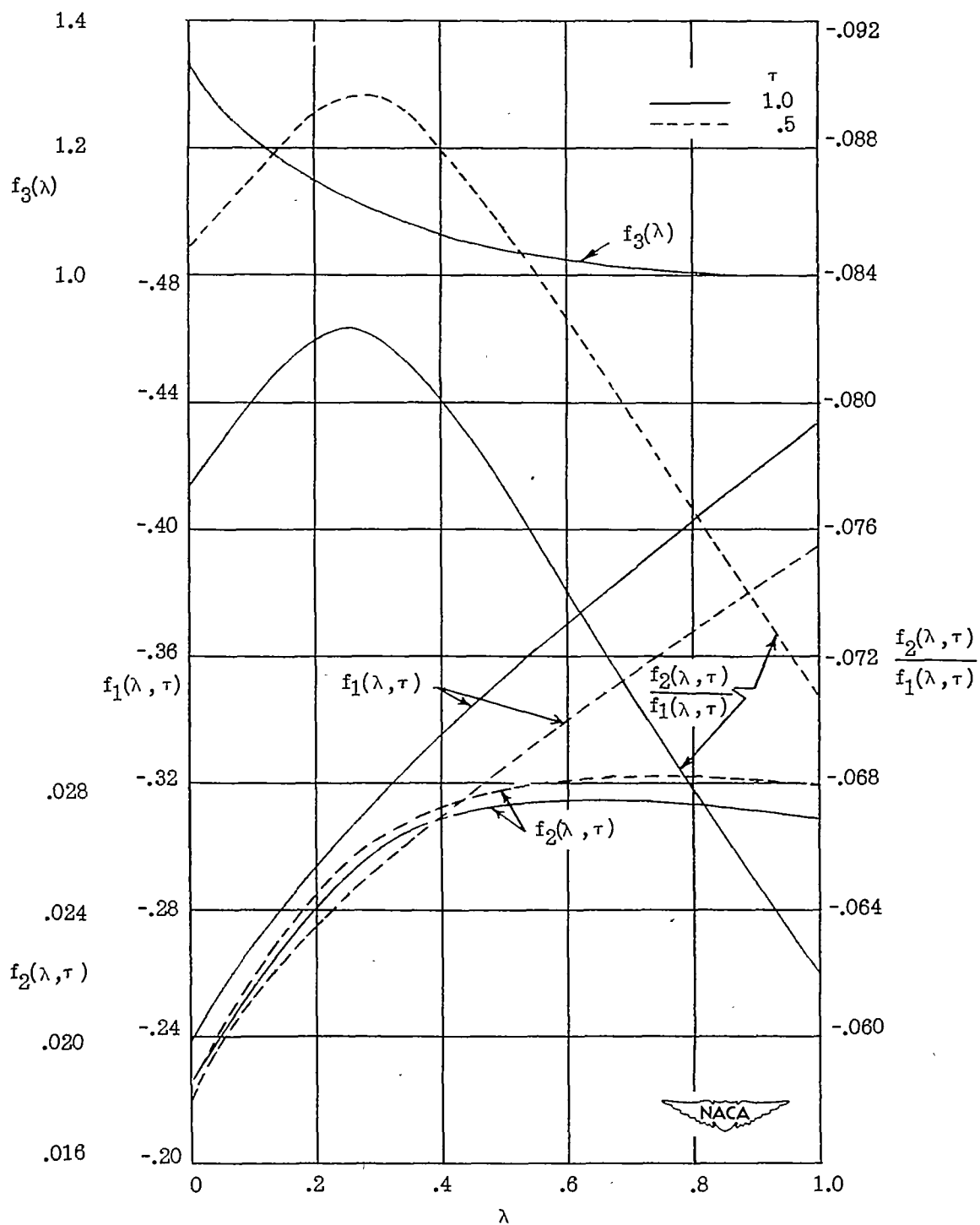
Figure 7.- Variation with taper ratio of various functions pertinent to
the analysis of aeroelastic effects.
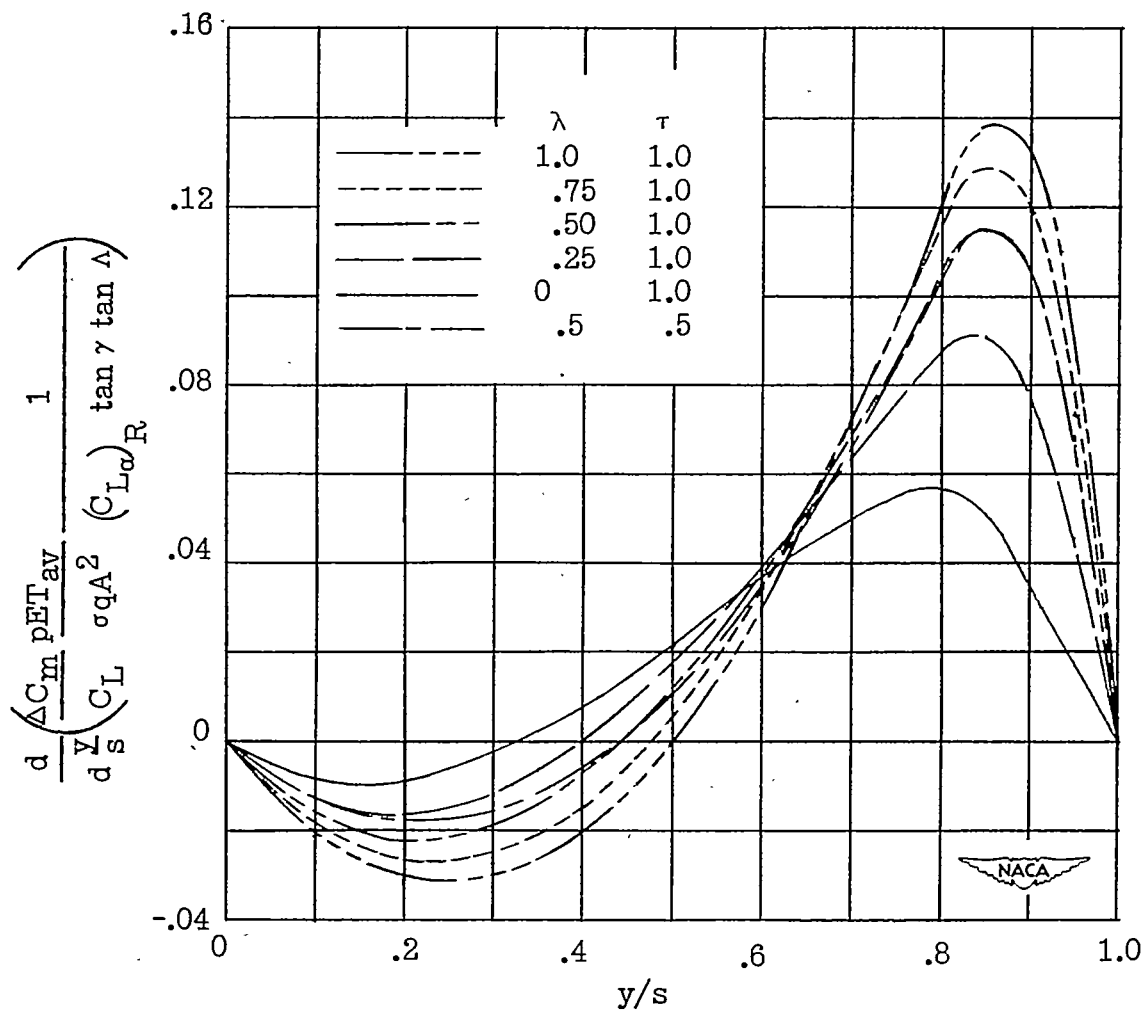
Figure 8.- Typical spanwise variation of the pitching moment produced by wing bending for various plan-form and thickness taper ratios.
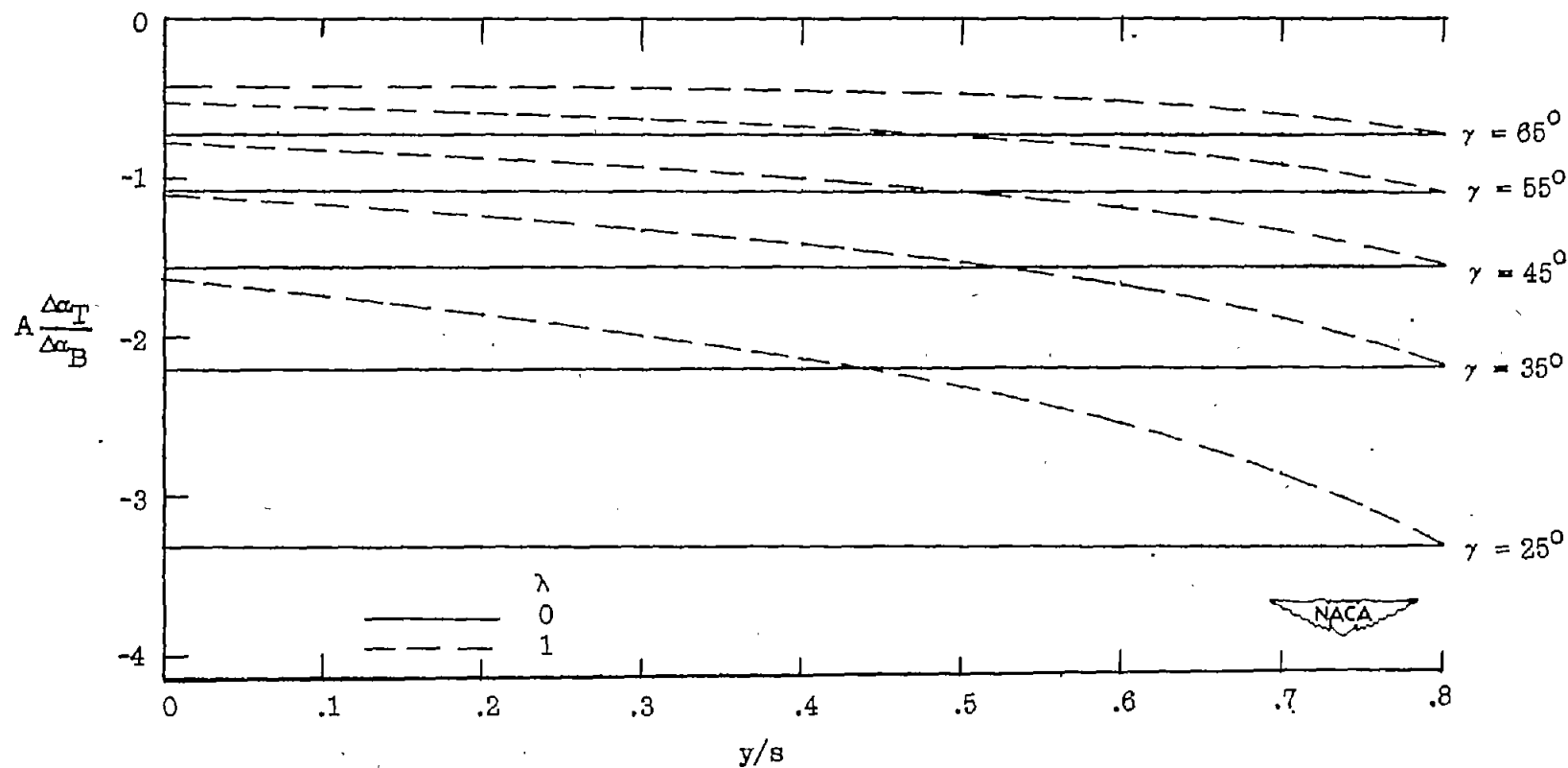
Figure 9.- The variation along the span of the ratio of the angle-of-attack change produced by wing torsion to the angle-of-attack change produced by wing bending. $\frac{J}{I} = 3.5$; e = 0.25.

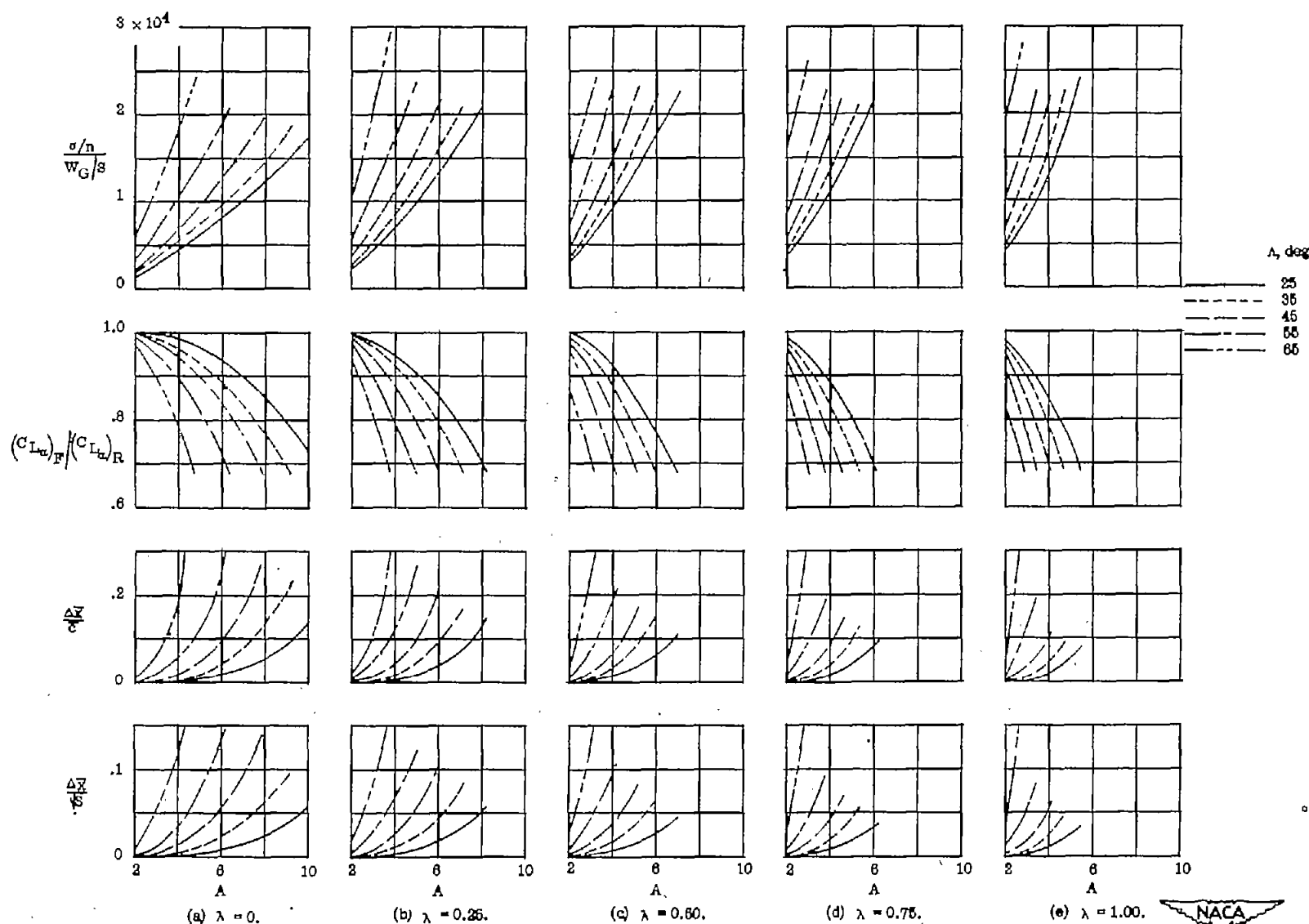(a) T = 0.04.   (b) T = 0.08.   (c) T = 0.12.
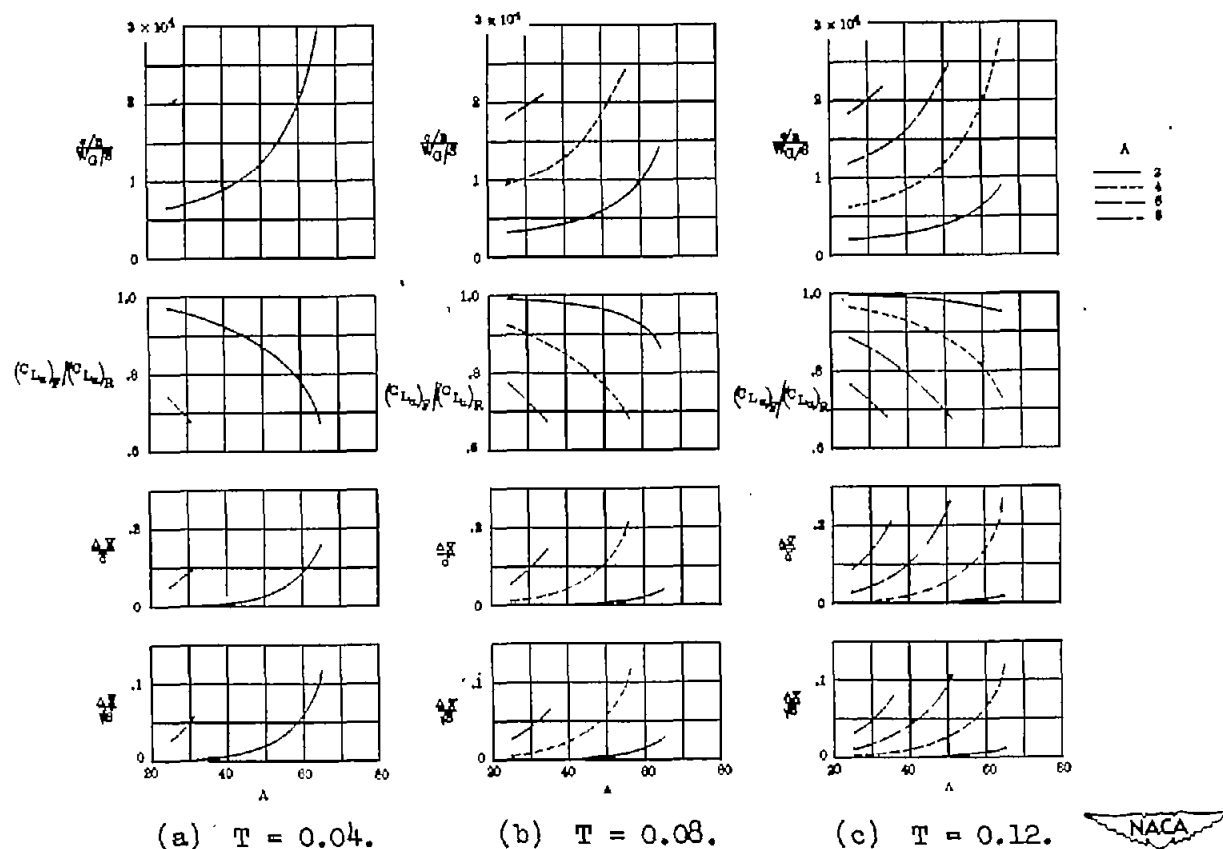
Figure 10.- Variation with angle of sweepback of bending stress per g normal acceleration, ratio of lift-curve slopes of flexible and rigid wing, and shift in aerodynamic center due to bending showing effects of aspect ratio, sweepback angle, and thickness ratio. Duralumin wings; plan-form taper ratio 0.5; constant thickness ratio along span; symmetric parabolic-arc section; structural weight $\frac{W}{S^{3/2}} = 0.2$; Mach number, 0.9; altitude, 30,000 feet.

Figure 11.- Variation with aspect ratio of bending stress per g normal acceleration, ratio of lift-curve slopes of flexible and rigid wing, and shift in aerodynamic center due to bending for various sweepback angles showing effect of plan-form taper ratio. Duralumin wings; constant section thickness ratio of 0.03; symmetric parabolic-arc section; structural weight $\frac{W}{S^{3/2}} = 0.2$; Mach number, 0.9; altitude, 30,000 feet.
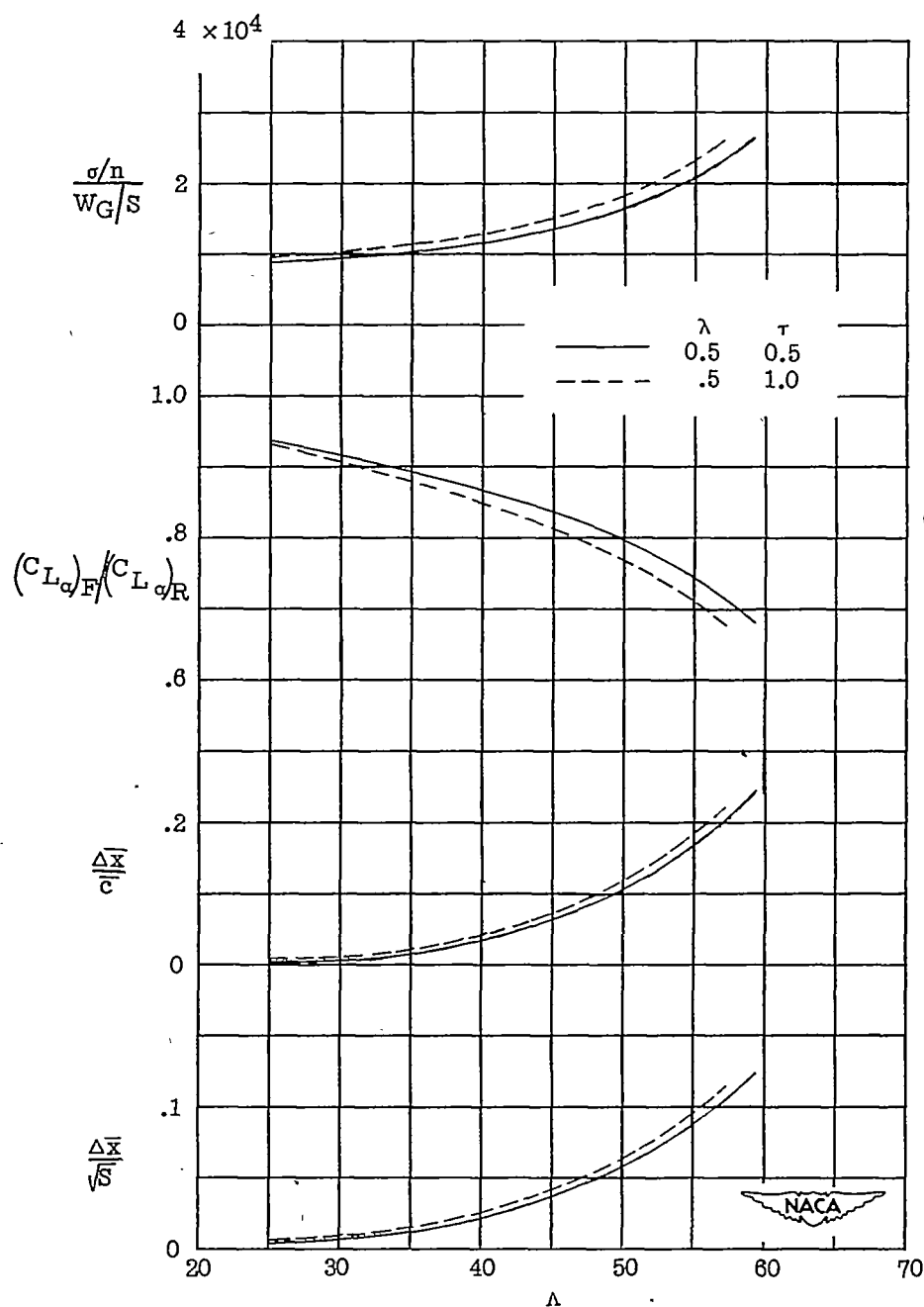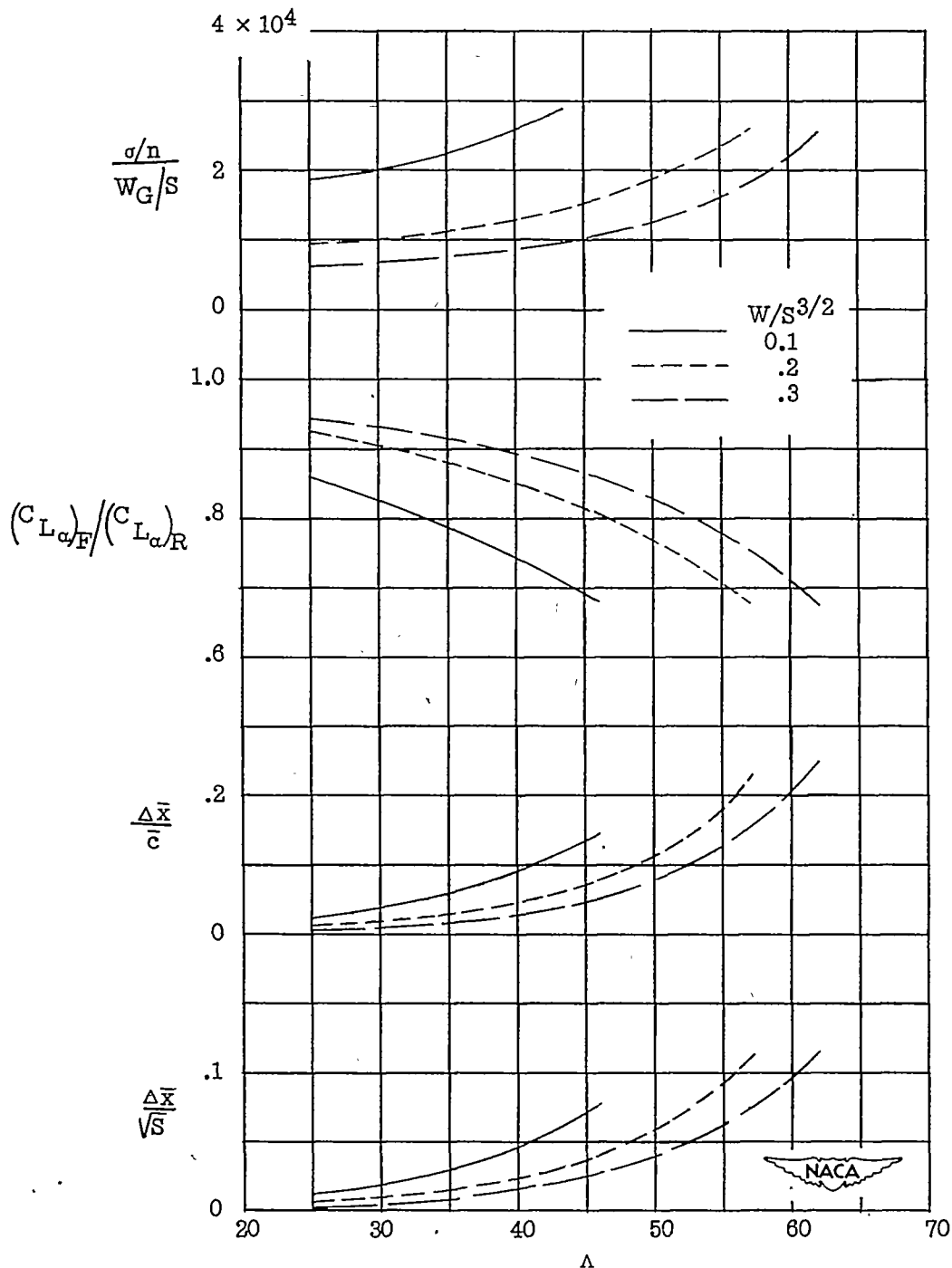
Figure 12.- Variation with angle of sweepback of stress per g normal
   acceleration, ratio of lift-curve slopes of flexible and rigid wing,
   and shift in aerodynamic center due to bending for thickness taper
   ratios of 1.0 and 0.5. Duralumin wings; aspect ratio 4; thickness
   ratio 0.08 (average of the root and tip section thickness ratios);
   plan-form taper ratio 0.5; symmetric parabolic-arc section; struc-
   tural weight $\dfrac{W}{S^{3/2}}$ = 0.2; Mach number, 0.9; altitude, 30,000 feet.
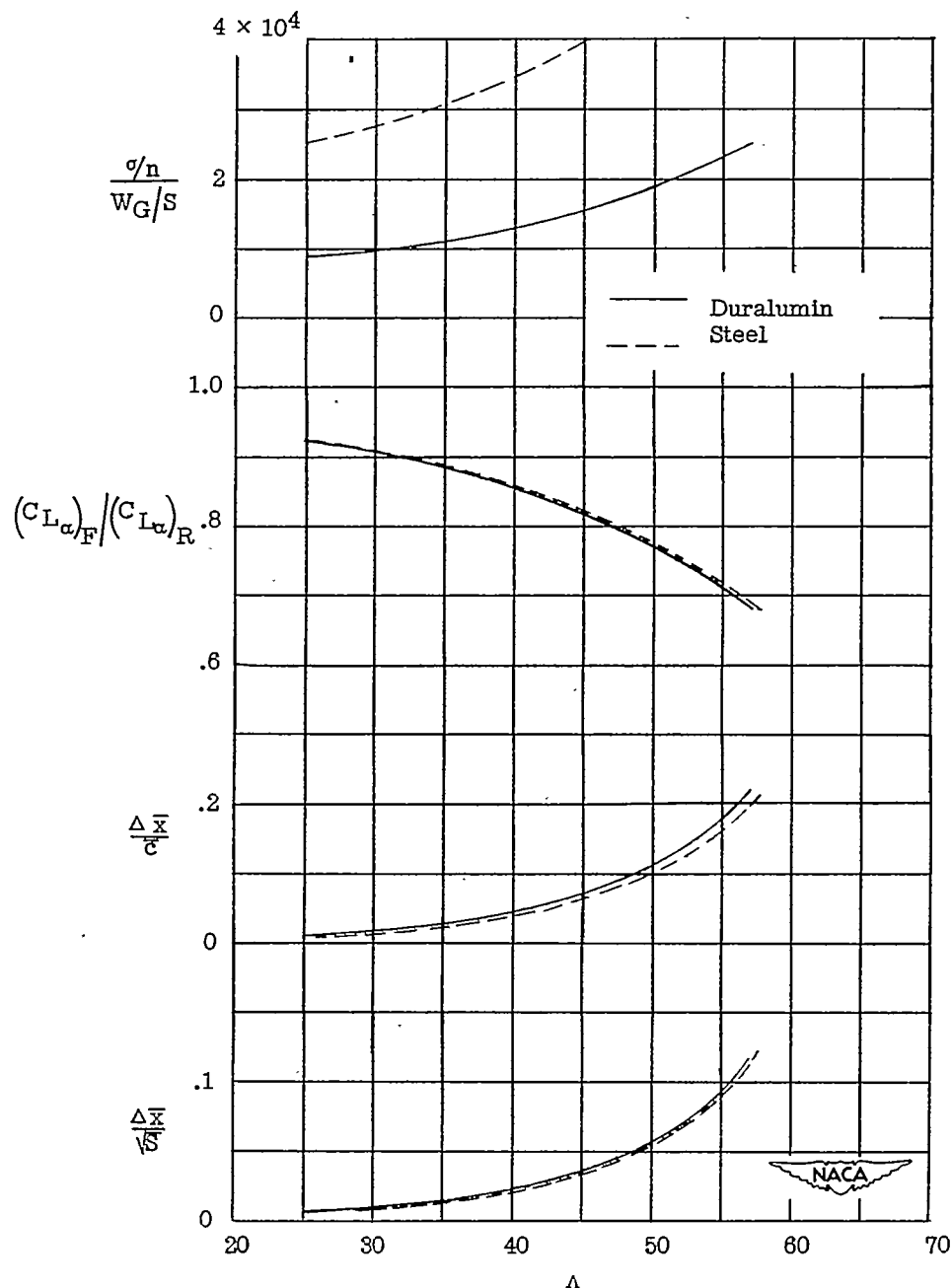
Figure 13.- Variation with angle of sweepback of stress per g normal
  acceleration, ratio of lift-curve slopes of flexible and rigid wing,
  and shift in aerodynamic center due to bending showing effect of
  structural weight.   Duralumin wings; aspect ratio 4; constant thick-
  ness ratio of 0.08; plan-form taper ratio 0.5; symmetric parabolic-
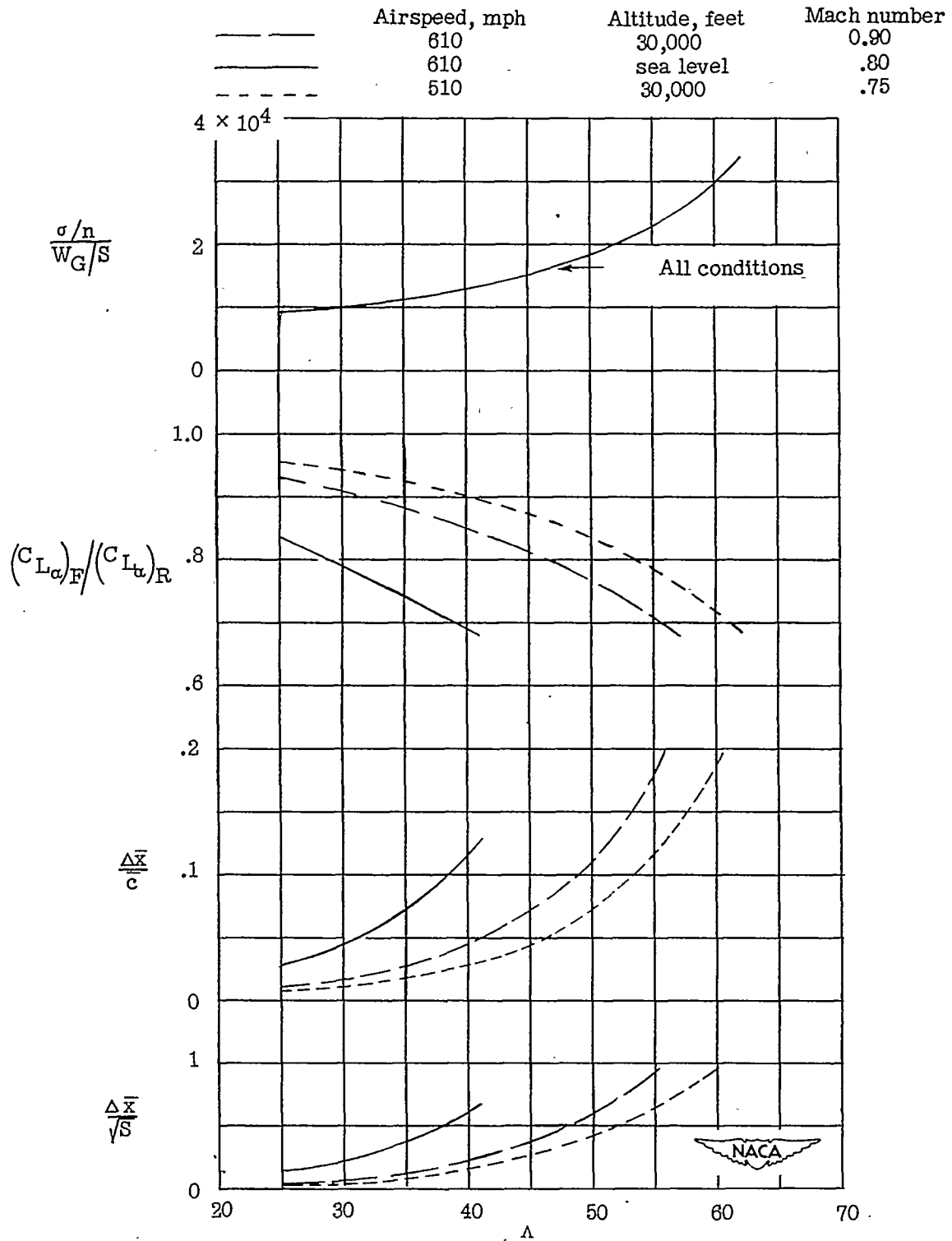 arc section; Mach number, 0.9; altitude, 30,000 feet.

Figure 14.- Variation with angle of sweepback of stress per g normal
   acceleration, ratio of lift-curve slopes of flexible and rigid wing,
   and shift in aerodynamic center due to bending showing effect of
   choice of steel or duralumin as structural material. Aspect ratio 4;
   constant thickness ratio of 0.08; plan-form taper ratio 0.5; sym-
   metric parabolic-arc section; structural weight $\dfrac{W}{s^{3/2}}$ = 0.2; Mach

   number, 0.9; altitude, 30,000 feet.

	Airspeed, mph	Altitude, feet	Mach number
— — —	610	30,000	0.90
————	610	sea level	.80
– – – –	510	30,000	.75

Figure 15.- Variation with angle of sweepback of stress per g normal
acceleration, ratio of lift-curve slopes of flexible and rigid wing,
and shift in aerodynamic center showing effect of flight condition.
Duralumin wings; aspect ratio 4; constant thickness ratio of 0.08;
plan-form taper ratio 0.5; symmetric parabolic-arc section; struc-
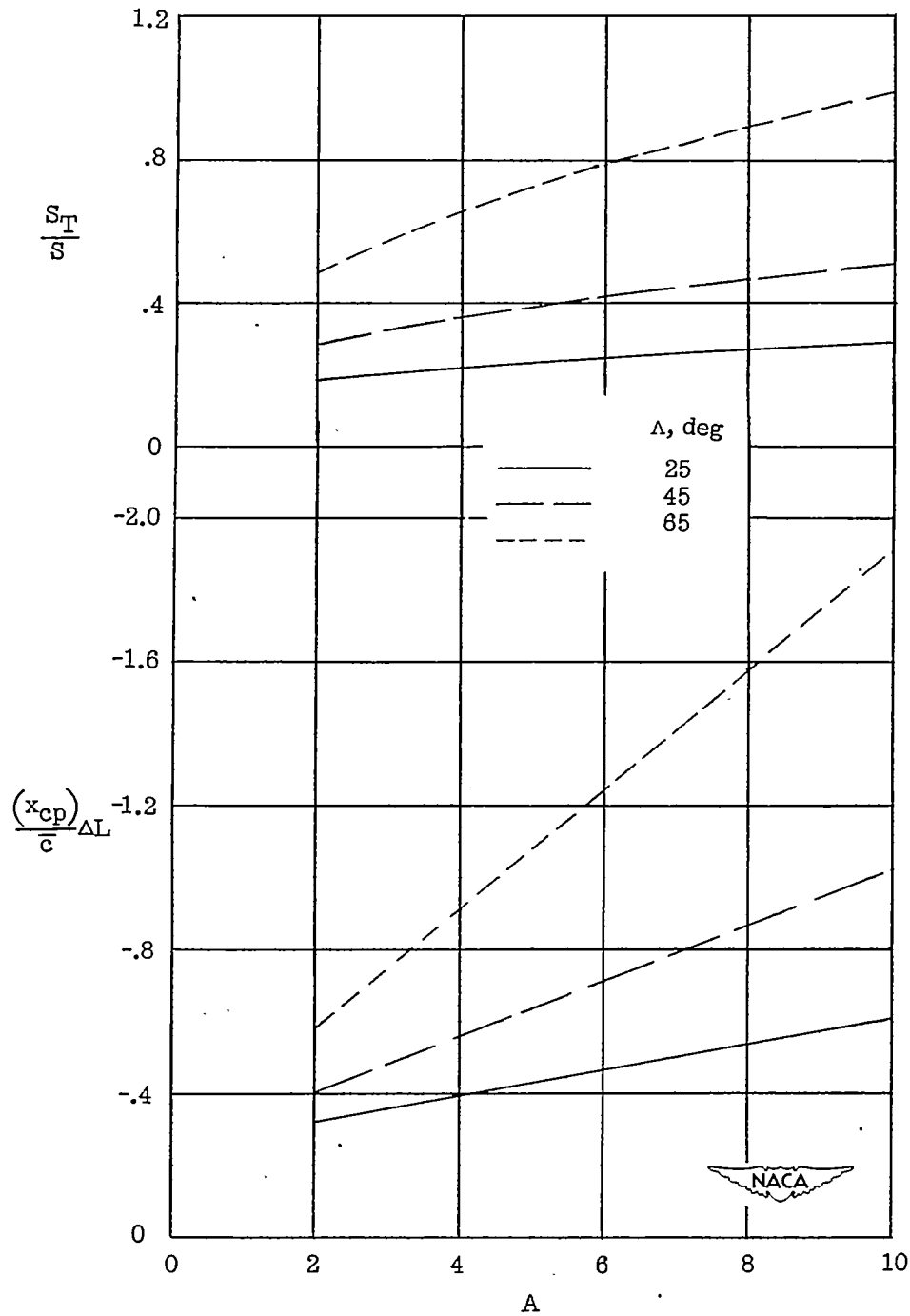tural weight $\dfrac{W}{S^{3/2}} = 0.2$.

Figure 16.- Variations with aspect ratio of the center of pressure of
    the loss in lift due to wing bending and the tail area required to
    position the point for neutral static stability with respect to
    angle of attack at the center of pressure of the loss in lift when
    a rigid tail and fuselage are assumed. Wing taper ratio 0.5; con-
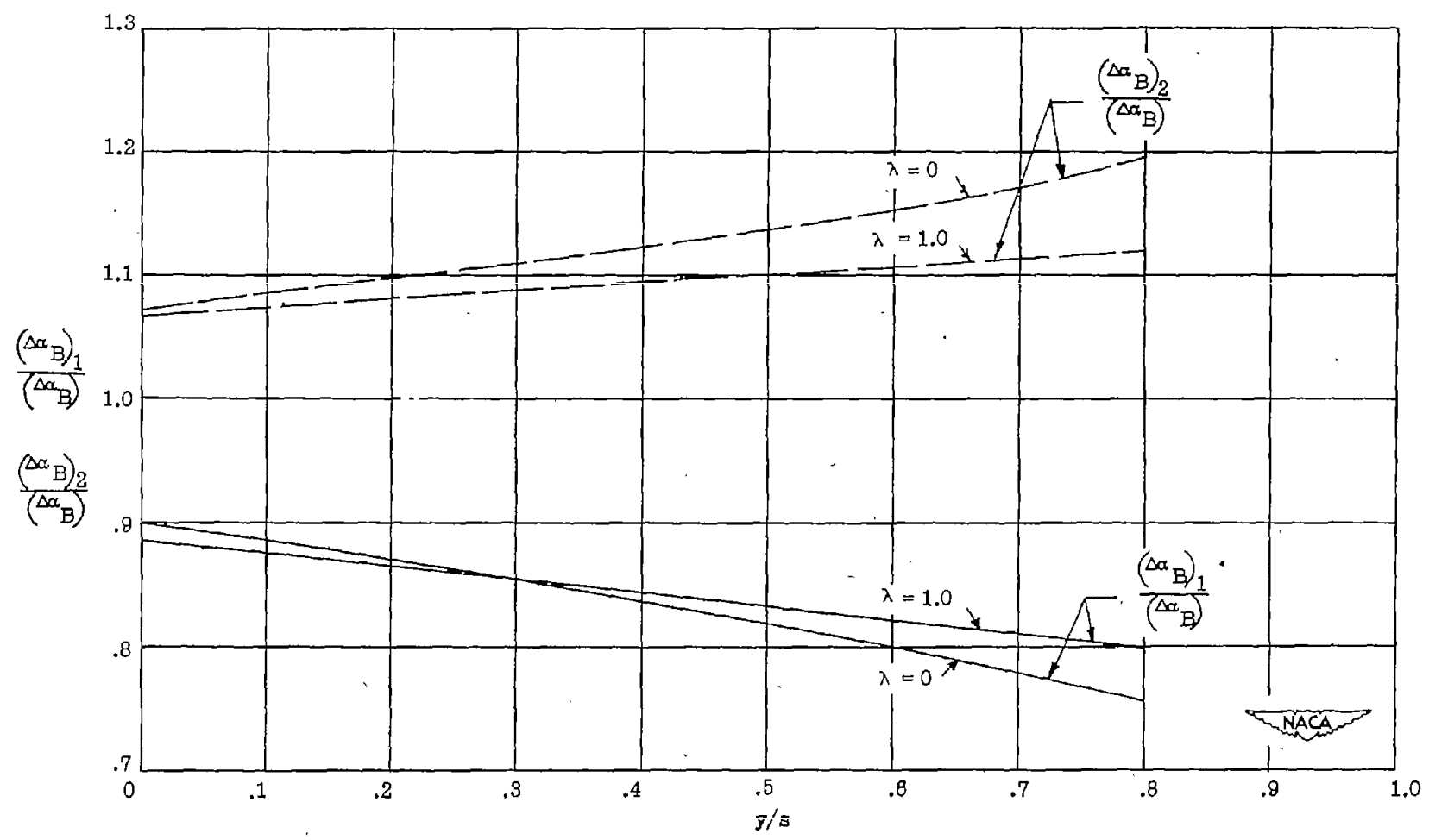   stant thickness ratio.

Figure 17.- Effect of distribution of loading on the spanwise variation
of angle of attack due to bending.